Earth's tectonic and plate boundary evolution over 1.8 billion years

Xianzhi Cao[1], Alan S. Collins[2], Sergei Pisarevsky[3], Nicolas Flament[4], Sanzhong Li[1], Derrick Hasterok[2], R. Dietmar Müller[5]

[1]Frontiers Science Center for Deep Ocean Multispheres and Earth System; Key Lab of Submarine Geosciences and Prospecting Techniques, MOE and College of Marine Geosciences, Ocean University of China, Qingdao 266100, China.

[2]Tectonics and Earth Systems & Mineral Exploration Cooperative Research Centre, School of Physics, Chemistry and Earth Sciences, The University of Adelaide, Adelaide, SA 5005, Australia.

[3]Earth Dynamics Research Group, School of Earth and Planetary Sciences, Curtin University, WA 6845, Australia.

[4]GeoQuEST Research Centre, School of Earth and Environmental Sciences, University of Wollongong, Northfields Avenue, NSW 2522, Australia.

[5]EarthByte Group, School of Geosciences, The University of Sydney, NSW 2006, Australia.

This paper is a non-peer reviewed pre-print that has been submitted to the journal Geoscience Frontiers for publication consideration.

Earth's tectonic and plate boundary evolution over 1.8 billion years

Xianzhi Cao[1], Alan S. Collins[2], Sergei Pisarevsky[3], Nicolas Flament[4], Sanzhong Li[1], Derrick Hasterok[2], R. Dietmar Müller[5]

[1]Frontiers Science Center for Deep Ocean Multispheres and Earth System; Key Lab of Submarine Geosciences and Prospecting Techniques, MOE and College of Marine Geosciences, Ocean University of China, Qingdao 266100, China.

[2]Tectonics and Earth Systems & Mineral Exploration Cooperative Research Centre, School of Physics, Chemistry and Earth Sciences, The University of Adelaide, Adelaide, SA 5005, Australia.

[3]Earth Dynamics Research Group, School of Earth and Planetary Sciences, Curtin University, WA 6845, Australia.

[4]GeoQuEST Research Centre, School of Earth and Environmental Sciences, University of Wollongong, Northfields Avenue, NSW 2522, Australia.

[5]EarthByte Group, School of Geosciences, The University of Sydney, NSW 2006, Australia.

Email: caoxianzhi@ouc.edu.cn; caoxianzhi1990@163.com

Abstract: Understanding the intricate relationships between the solid Earth and its surface systems in deep time necessitates comprehensive full-plate tectonic reconstructions that include evolving plate boundaries and oceanic plates. In particular, a tectonic reconstruction that spans multiple supercontinent cycles is important to understand the long-term evolution of Earth's interior, surface environments and mineral resources. Here we present a new full-plate tectonic reconstruction from 1.8 Ga to present that combines and refines three published models: one full-plate tectonic model spanning 1 Ga to present, and two continental-drift models focused on the late Paleoproterozoic to Mesoproterozoic eras. Our model is constrained by geological and geophysical data, and presented as a relative plate motion model in a palaeomagnetic reference frame. The model encompasses three supercontinents, Nuna (Columbia), Rodinia, and Gondwana/Pangea, and more than two complete supercontinent cycles, covering ~40% of the Earth's history. Our refinements to the base models are focussed on times before 1.0 Ga, with minor changes for the Neoproterozoic. For times between 1.8 Ga and 1.0 Ga, the root mean square speeds for all plates range between 4 and 10 cm/yr, and the net lithospheric rotation is below 0.9°/Myr, which are kinematically consistent with post-Pangean plate tectonic constraints. The time spans of the existence of Nuna and Rodinia are updated to between 1.6 Ga (1.65 Ga in the base model) and 1.46 Ga, and between 930 Ma and 780 Ma (800 Ma in the base model), respectively, based on geological and paleomagnetic data. We follow the base models to leave Amazonia/West Africa separate from Nuna (as well as Western Australia, which only collides with the remnants of Nuna after initial break-up), and South China/India separate from Rodinia. Contrary to the concept of a "boring billion", our model reveals a dynamic geological history between 1.8 Ga and 0.8 Ga, which is characterized by supercontinent assembly and breakup, continuous accretion events,

and widespread LIP events. The model is publicly accessible, providing a framework for future refinements and facilitating deep time studies of Earth's system.

Keywords: Plate reconstruction, Nuna, Supercontinent, Proterozoic, Palaeogeography

1. Introduction

The motion and recycling of tectonic plates shapes the long-term evolution of the Earth's surface and affects deep mantle convection patterns (e.g. Flament et al., 2022; Müller et al., 2022a; Nance et al., 2014). Reconstructing past plate tectonic configurations (Seton et al., 2023) is required to understand the deep-time controls and interactions between the solid Earth and the climate (e.g. Gernon et al., 2021; Goddéris et al., 2017; Mills et al., 2023), the carbon cycle (e.g. Goddéris et al., 2023; Müller et al., 2022b), the water cycle (Karlsen et al., 2019), the space and time distribution of critical mineral deposits (e.g. Wrobel-Daveau et al., 2022), the nutrient flux required to power biosphere evolution (e.g. Brocks et al., 2017; Cox et al., 2022; Mukherjee and Large, 2020; Spencer, 2022; Zhu et al., 2022) and elucidating the plate tectonic controls on paleogeography (e.g. Collins et al., 2021; Merdith et al., 2017b). Supercontinents, resulting from the aggregation of most continental crust into a single landmass, represent a fascinating phenomenon of plate tectonics. Two well-known Proterozoic supercontinents, Rodinia and Nuna (Fig. 1), have been subjects of extensive research, although their configurations are still the subject of much debate. The assembly of Rodinia was largely completed through global orogenesis at the end of the Mesoproterozoic (Evans, 2013). Major building blocks of the previous supercontinent Nuna (Hoffman, 1997), also sometimes named Columbia (Rogers and

Santosh, 2002), or Hudsonland (Williams et al., 1991), were formed over a protracted period of time spanning the middle to late Paleoproterozoic (Zhao et al., 2002). Recently, geochronological and paleomagnetic studies have constrained the final assembly of Nuna between western North America and eastern Australia to ~1.6 Ga (Kirscher et al., 2022; Pourteau et al., 2018).

In the absence of preserved ocean floor, reconstructions of the pre-Pangean Earth rely on geological evidence preserved within the continents. Age-equivalent orogenic belts, dyke intrusions, comparable rift histories and provenance records, are crucial data to establish past relationships between continents, or constrain supercontinent configurations, especially for early studies (Rogers and Santosh, 2002; Zhao et al., 2002). With the accumulation of paleomagnetic data in recent years, significant progress has been made in building quantitative kinematic reconstructions through time. Early kinematic reconstructions focussed on modelling continental motions without plate boundaries or oceanic plates (Eglington et al., 2013; Li et al., 2008; Pisarevsky et al., 2014) due to the lack of data and technical difficulties in building reconstructions with time-dependent plate geometries.

Plate tectonic reconstructions that include evolving global plate boundaries, also called full-plate reconstructions (Merdith et al., 2017a), have become possible with the development of the software GPlates (Müller et al., 2018). Several such models have been published over the last decade, covering different time periods and based on varying geological or geophysical datasets (Merdith et al., 2021). The earliest of these are for post-Pangea times (Müller et al., 2016; Seton et al., 2012), and later for the Paleozoic (e.g. Domeier and Torsvik, 2017). Merdith et al. (2021) created a breakthrough model spanning 1 Ga to present, building on, and integrating, previous models. Li et al. (2023) published a model for the period of 2.0 Ga to 540 Ma, through modifying and extending their previous Rodinia model (Li et al., 2008) further back in time and incorporating elements of evolving plate margins. For the pre-Pangean period, whole Earth plate reconstructions rely on extrapolation of available observations from continents, which introduces relatively larger uncertainties. Paleomagnetic data play a particularly important role in this context (e.g. Kirscher et al., 2022; Li et al., 2023; Li et al., 2008; Meert and Santosh, 2022; Pisarevsky et al., 2014). However, in addition, the geological record preserved in the continents preserves vast untapped information regarding the tectonic geography of the planet through time (Seton et al., 2023). Integrating these geological data with necessarily limited paleomagnetic information provides testable predictions for regions and time periods for which direct observations are lacking, especially when combined with empirically observed 'rules' of plate tectonics (e.g. Müller et al., 2022a). The resulting models, although still non-unique, enable quantitative estimates of tectonic processes and provides insights into the connections between the deep Earth and its surface (Cao et al., 2021; Flament et al., 2022; Müller et al., 2022a).

The operation of plate tectonics prior to the middle Neoproterozoic is debated. An interpretation of geological phenomena that suggest elevated mantle temperatures during this time (Brown et al., 2020; Tamblyn et al., 2022), suggests that the Earth might have been in a 'stagnant lid' regime with limited lateral movement of plates during mid-Neoproterozoic times (Stern, 2018). In contrast, Roberts et al. (2022) interpreted the same metamorphic gradients as compatible with a tectonic regime similar to the modern one, with relatively rigid lithospheric plates moving laterally relative to each other and subducting into the mantle. The relative stability and longevity of a large supercontinent through much of the mid Neoproterozoic times could have locally elevated mantle temperatures through insulation (Brown et al., 2022; Gurnis, 1988; Tamblyn et al., 2022; Zou et al., 2023).

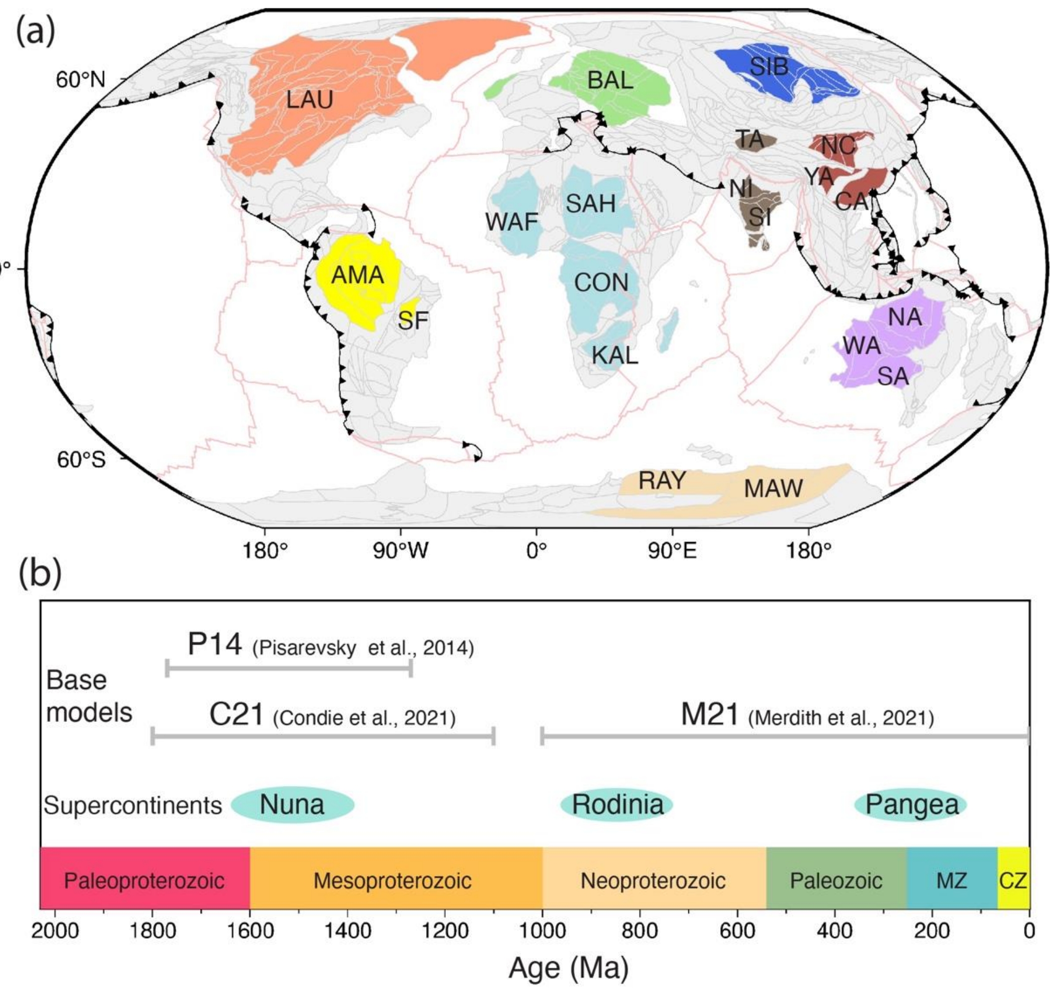

Fig. 1. (a) Major cratonic blocks used in the reconstruction before 1.0 Ga; (b) The three base models used in this study. The grey lines in (b) show the timespan of each base model. Our new model includes three supercontinents: Nuna, Rodinia and Pangea. LAU-Laurentia, AMA-Amazonia, SF-São Francisco, BAL-Baltica, RAY-Rayner Province, MAW-Mawson, SA-South Australia, NA-North Australia, WA-West Australia, YA-Yangtze, CA-Cathaysia, NC-North China, SIB-Siberia, TA-Tarim, SI-South India, NI-North India, CON-Congo, KAL-Kalahari, WAF-West Africa, SAH-Sahara Metacraton.

Despite the recent advancements in modelling continental motions and plate boundary evolution, the construction of a continuous tectonic model, constrained by geological and high-quality paleomagnetic data and connecting the Phanerozoic and Mesoproterozoic, encompassing all three well-known supercontinents (Nuna, Rodinia, Pangea), has remained elusive. Li et al. (2023) introduced a paleomagnetic-focused reconstruction encompassing Nuna and Rodinia supercontinents. Here, we present a considerably different, new topological full-plate plate model spanning 1.8 Ga to the present day, through merging and updating previously published models and focussing particularly on the geological relationships between plates, as well as considering geophysical (e.g. paleomagnetic) constraints.

2. Methods

2.1 Model construction

Our 1.8 Ga–present full-plate reconstruction is built based on three published models (Fig. 1b) using GPlates (Müller et al., 2018). The model of Pisarevsky et al. (2014, referred to as P14) is the base model for times before 1.0 Ga, for which the model by Condie et al. (2021, referred to as C21) is also used. P14 and C21 are similar late Paleoproterozoic–Mesoproterozoic models with small differences: P14 has slightly smaller time intervals (~ 20–70 Myr) compared to C21 (100 Myr). Additionally, C21 covers a longer timespan (1800–1100 Ma) compared to P14 (1770–1270 Ma). For the period from 1.0 Ga to present, we adopt the model from Merdith et al. (2021, referred to as M21), with minor adjustments made for the Neoproterozoic era. All three models are global plate models, extensively constrained by geological and geophysical data. P14 and C21 are "continental-drift" type models, lacking plate boundaries and oceanic plates, while M21 includes both continental blocks and a dynamic network of evolving plate boundaries.

The construction of our model involves the following steps. We first create a new model for the period 1800–1100 Ma by combining P14 and C21. Specifically, we use P14 for the time range of 1770–1270 Ma and employ C21 for the remaining time intervals. We subsequently link this 1800-1100 Ma model to M21. To ensure a seamless transition, we introduce additional finite rotations based on available data for the period 1100–1000 Ma that is not covered by either base model. We then update the model (e.g. improve the match of plates to paleomagnetic poles, adjust the timings of collisions and rift events) by incorporating new paleomagnetic and geological data. Lastly, we construct continuous plate boundaries, primarily focusing on the 1800–1000 Ma period.

We use the continental outlines from model M21 and make minor modifications to the continents that consisted of relatively small separate blocks before 1000 Ma (Fig. 1a). For example, Baltica is a single landmass in M21, but is divided into multiple small blocks in our model. Earth's surface before Nuna was characterized by numerous micro-continents (Li et al., 2018). The cratonic core of most continents formed in the late Paleoproterozoic (Zhao et al., 2002), with additional continental growth during Mesoproterozoic accretionary orogenies, such as those in Laurentia and Baltica (e.g. Condie et al., 2021; Whitmeyer and Karlstrom, 2007). Our reconstruction before 1.0 Ga includes most major cratonic blocks (refer to Fig. 1 here and Fig. 10 in Hasterok et al., 2022), with the exception of a few small blocks (e.g. the Rio de la Plata craton) due to limited data availability. We do not extend our model deeper in time than 1.8 Ga due to extensive continental fragmentation before this time (e.g. Zhao et al., 2002).

We build a relative plate motion model, similar to M21. The motions of all continents in P14 and C21 are constrained by paleomagnetic data and therefore directly tied to the paleomagnetic reference frame. We recalculate the equivalent rotations of all blocks relative to an adjacent plate, incorporating them into a relative plate motion hierarchy while preserving their overall absolute motion. This conversion to a relative plate motion model is important when using geological data to model the relative motion of plates. It also facilitates future testing of alternative absolute reference frames, such as the no-net-lithospheric-rotation frame, by maintaining the relative plate motions. We highlight the utility of this approach as plate-tectonic phenomena responsible for lithospheric and earth-surface system evolution are controlled by plate interactions rather than their relationship to Earth's magnetic field.

During the existence of Rodinia, Laurentia is used as the base of the plate hierarchy in M21 due to its central position within the supercontinent. Although Laurentia was not located at the centre of Nuna, we establish plate motion chains primarily tying most plates to Laurentia both for consistency and because it is the best-constrained continent for this time period. Laurentia is linked to Earth's spin axis through a paleomagnetic reference frame. The motions of plates within superoceans are tied to triple junctions, similar to the evolution of the Pacific ocean basin since the Jurassic (Seton et al., 2012), or the Panthalassan plates in the Late Paleozoic (Young et al., 2019).

2.2 Paleomagnetic poles

Paleomagnetic data provide quantitative information about continental paleolatitudes and their azimuthal orientation. We compile 204 paleomagnetic poles with ages > 600 Ma (including 150 poles > 1000 Ma, Table. S1 and Fig. 2) from the GPMDB database (http://gpmdb.net; Pisarevsky et al., 2022) to determine the paleolatitudes of continents. While there are good data coverage for a few continents, including Laurentia, Baltica, North China, and North Australia, data are sparse or limited for some other continents. For example, there are no paleomagnetic poles for South China and Tarim older than 1.0 Ga, and there is only one such pole for West Africa. We use the poles to refine the base models or include continents that are not included in the based models.

The geological record can also be used to constrain tectonic evolution. Age-dated tectonic phenomena, such as orogeny, rifting and magmatism, provide valuable insights into the relative motion of plates and the timing of geological events. Plate kinematic rules (e.g. plate speeds), inferred from post-Pangea plate motions, serve as a guide for earlier plate motions (Müller et al., 2022a).

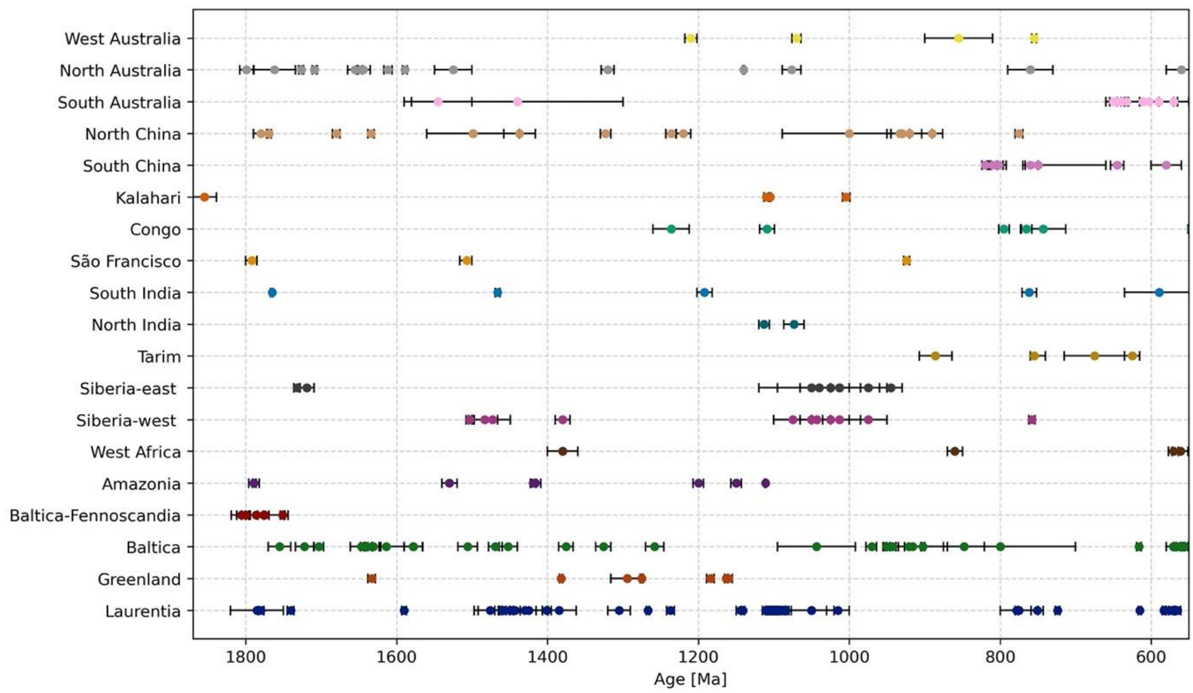

Fig. 2. Temporal distribution of the paleomagnetic poles used in this study. The poles are compiled from the GPMDB database (http://gpmdb.net; Pisarevsky et al., 2022). Baltica here indicates eastern Baltica (i.e. Sarmatia/Volgo-Uralia) before 1.7

Ga and the whole of Baltica (Sarmatia/Volgo-Uralia and Fennocandia) afterwards. The error bars show the age uncertainties of the poles.

There currently exists no widely accepted method to constrain paleolongitude of plates. An approach has been suggested to reconstruct large igneous provinces (LIPs) and kimberlites as well as the plates carrying them, to align with the edges of Large Low Shear Velocity Provinces (LLSVPs, Garnero and McNamara, 2008; Torsvik and Cocks, 2017). This approach assumes that the LLSVPs are fixed, and LIPs and kimberlites are the product of plumes rising along LLSVP edges (Burke et al., 2008; Torsvik et al., 2010). However, geodynamic models and seismic observations suggest that LLSVPs are deformable through interaction with cold slabs (Flament et al., 2022; Frost and Rost, 2014; Zhang et al., 2010). Furthermore, statistical analyses show that it cannot be distinguished whether the LIPs and kimberlites are correlated with LLSVP margins or with their interiors (Austermann et al., 2014; Davies et al., 2015).

Mitchell et al. (2012) used paleomagnetic data to propose an “orthoversion” model, in contrast to previously proposed “introversion” and “extroversion” models (Murphy and Nance, 2003), in which a new supercontinent assembles over the downwelling subduction girdle of the previous supercontinent, and two successive supercontinents are spatially ca. 90° away from each other. The longitudinal movements in our model are primarily derived from the base models, with small adjustments made to reduce plate velocities and ensure a smoother transition to model M21. In our model, Nuna (based on P14) is about 105° away from Rodinia (largely derived from M21), which is broadly compatible with “orthoversion”.

2.3 Identification of plate boundary types

Metamorphic and geochemical data between 1850–800 Ma from Hasterok et al. (2022) are used to identify different tectonic environments (Fig. 3). Four thousand seven hundred ages of igneous rocks, which are both I-type (derived from igneous protoliths) (Chappell and White, 1974), and magnesian-type (magnesian riched) of frost1 classification (Frost et al., 2001), are used to indicate potential subduction. Around 190 of metamorphic gradients with age constraints are also compiled (Brown and Johnson, 2018; Hasterok et al., 2022; Tamblyn et al., 2021). High metamorphic gradients (> 775 K/GPa) are used to identify potential rifting, low metamorphic gradients (< 375 K/GPa) indicate potential subduction, and medium metamorphic gradients (between 375 K/GPa and 775 K/GPa) indicate potential orogenesis due to continental thickening. Other geological data, for instance terrane accretion records (Fig. 4, Table S2), are also used to build subduction zones.

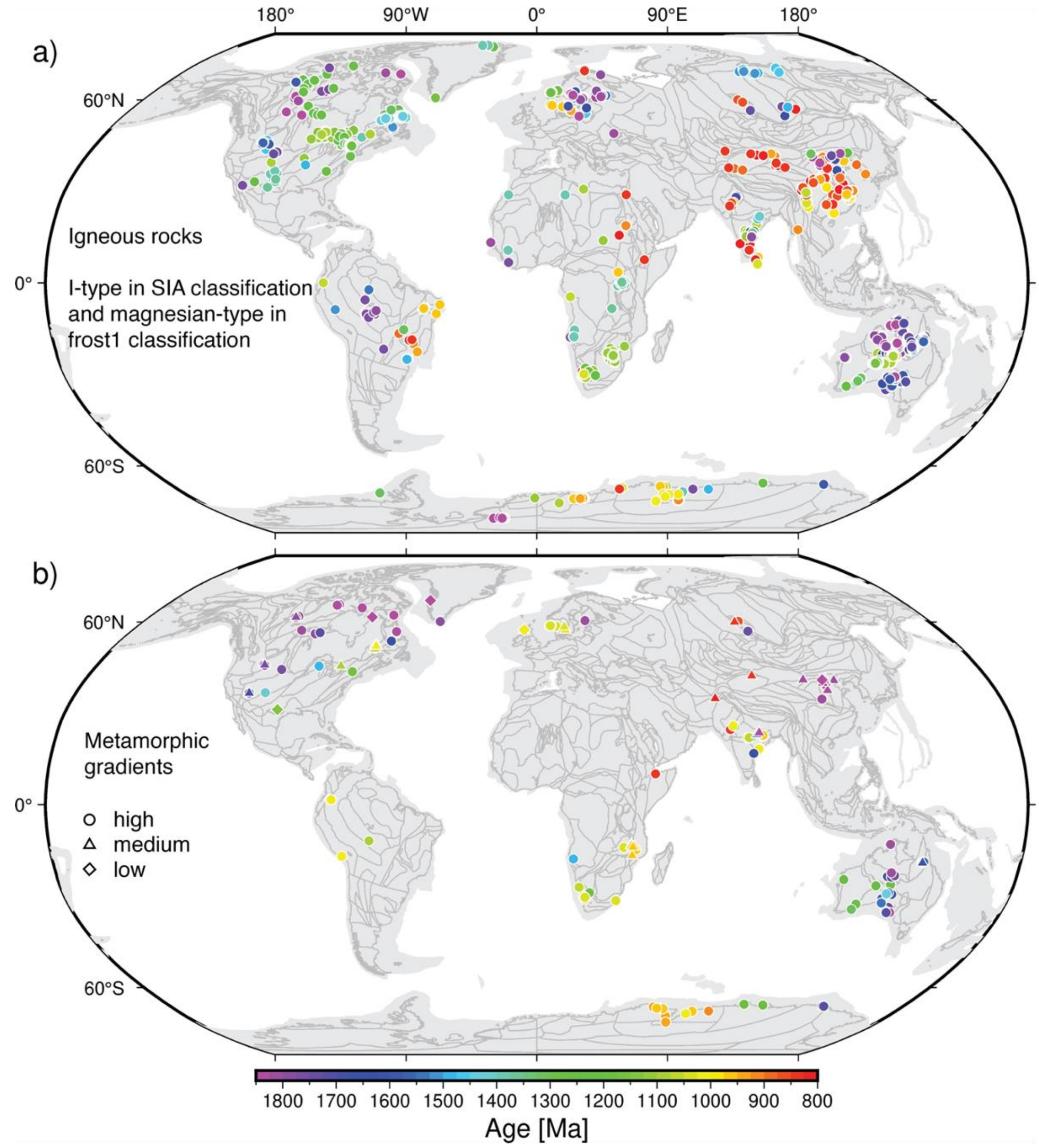

Fig. 3. Point data used for identifying plate boundary type. (a) igneous rocks of both I-type and magnesian-type of frost1 classification, (b) metamorphic gradients with age constraints, circles indicate high gradients (>775 K/GPa), triangles indicate medium values (375-775 K/GPa), and diamonds indicate low values (<375 K/GPa).

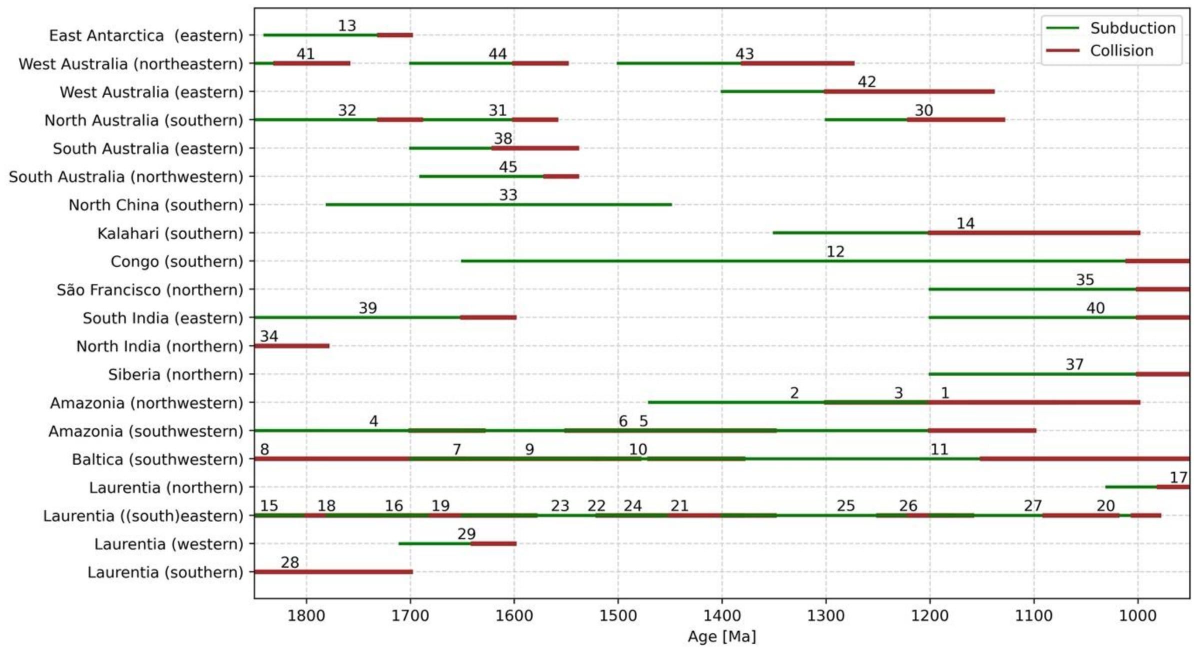

Fig. 4. Accretionary events along the margins of major cratonic blocks between 1.8 Ga and 1.0 Ga. The texts in brackets after cratonic block names denote along which margin the accretionary events occurred. The data are mainly from Condie et al. (2021) with minor changes (see Table S2). The numbers above the lines denote tectonic event numbers listed in Table S2. There are overlaps between different tectonic events indicating they occur in different segments of the margin, or due to age uncertainties.

Plate boundaries are more accurately constrained along continental margins with better-preserved geological records. Determining plate boundaries away from continents is challenging due to the lack of preserved ocean basins before the Mesozoic. In such cases, boundaries are inferred by connecting constrained boundaries or interpreting continental block motions. To maintain overall model consistency, some oceanic-only plates are introduced. For instance, a simple three-plate spreading scenario is implemented to ensure circum-Nuna subduction. These ridges and transforms are synthetic, but with a reasonable spreading rate. Boundaries are iteratively constructed to ensure alignment with plate motion patterns, and consistency with other boundaries.

3. Input models and modifications

P14 (the base model before 1 Ga) is based on a compilation of reliable paleomagnetic data (available before 2014), and also constrained by geological observations. In P14, Nuna formed around 1650–1580 Ma by joining at least two stable continental landmasses formed by ca. 1.7 Ga: West Nuna and East Nuna. West Nuna includes Laurentia, Baltica and India. East Nuna includes North, West and South Australia, the Mawson craton of Antarctica and North China. Siberia and the Congo/São Francisco craton were tentatively proposed as a third rigid continental entity that merged into Nuna at 1500 Ma. Amazonia-West Africa was located outside of Nuna. The breakup of Nuna occurred around 1460–1380 Ma, with East and West Nuna rifting apart.

M21 is a model spanning from 1 Ga to the present-day that combined several models for different time periods. At 1 Ga, M21 starts with most blocks (such as Laurentia, Baltica, Siberia, Amazonia, West Africa and some micro-blocks) being together. Australia, Mawson and North China were separated from these blocks by a transform boundary, and then joined Laurentia and other continents around 930 Ma to form Rodinia through dextral shearing. In this model, the breakup of Rodinia occurred at 800 Ma, resulting in the separation of Australia, Mawson, and North China from Laurentia, and the opening of the Proto-Pacific Ocean (Merdith et al. 2017b). Subsequently, Gondwana began to assemble around 520 Ma.

The majority of the modifications we have made to the base models are to the late Paleoproterozoic–Mesoproterozoic eras (models P14 and C21, Fig. 5). Our refinements to M21 are limited to the Neoproterozoic era, as follows.

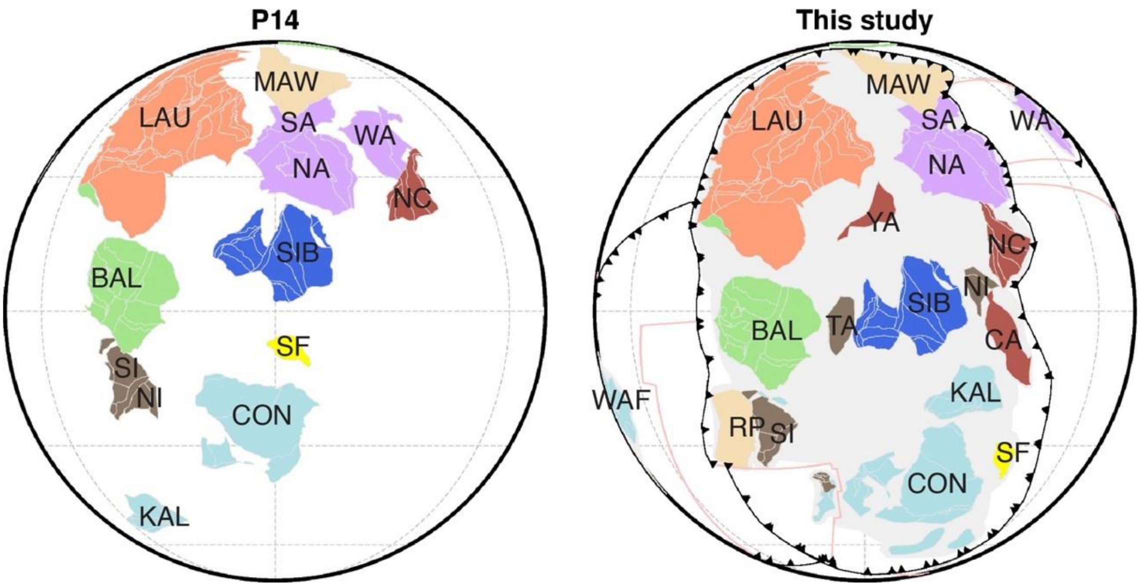

Fig. 5. The configuration of supercontinent Nuna (1580 Ma) in P14 and in this study. India is separated into the North Indian and South Indian blocks; Yangtze, Cathaysia and Tarim are added to our model; The positions of Siberia, Kalahari, North China, West Australia are adjusted based on paleomagnetic and geological data.

3.1. Nuna assembly and existence (1800–1460 Ma)

3.1.1 West Nuna (Laurentia, Baltica, South India, Yangtze)

Laurentia comprises several cratonic blocks, most of which amalgamated during 2.0–1.8 Ga. The Wyoming craton accreted onto Laurentia around 1.78–1.72 Ga, after the Big Sky orogeny (Harms et al., 2004), which is represented in our model at 1.75 Ga. The late Paleoproterozoic to Mesoproterozoic evolution of Laurentia is well constrained by paleomagnetic poles from P14 (Fig. 6). Our modifications to Laurentia are minor and include: (1) smoothing the motion of Laurentia to eliminate fast plate movements (Fig. 7). In P14, Laurentia exhibited some zigzag motion (Fig. 7a), resulting in plate velocities up to 12 cm/yr between 1.5–1.4 Ga (Fig. 7b). The speed is reduced to ~2 cm/yr in our model. This adjustment is important as Laurentia is at the base of the plate hierarchy in our model, and its motion affects that of other plates; (2) incorporating the accretion of small terranes along the present-day southeast margin of Laurentia, which were not accounted for in P14 (Fig. 6). This accretion occurred mostly during the 1.8–1.7 Ga Yavapai, the 1.7–1.6 Ma Mazatzal, and the 1.3–0.9 Ma Grenville orogenies (e.g. Karlstrom et al., 2001). (3) Adjusting the plate positions to better align with paleomagnetic data (Fig. S1).

We follow P14 and some other previous studies (e.g. Salminen and Pesonen, 2007), to juxtapose Baltica with Laurentia in Nuna, which is supported by paleomagnetic data and similar late Paleoproterozoic to Mesoproterozoic accretion records. Baltica consists of two parts: south-eastern Baltica (Sarmatia/Volgo-Uralia) and western Baltica (Fennoscandia), which assembled along the Central Russian collision belt during 1.8–1.7 Ga (Bogdanova et al., 2008). The collision was loosely constrained between 1720 and 1650 Ma in P14. Recently published paleomagnetic data (Poles No. 9422 and 9921 in Table S1) that are adopted in our model constrain the collision to have occurred between 1734 Ma and 1697 Ma.

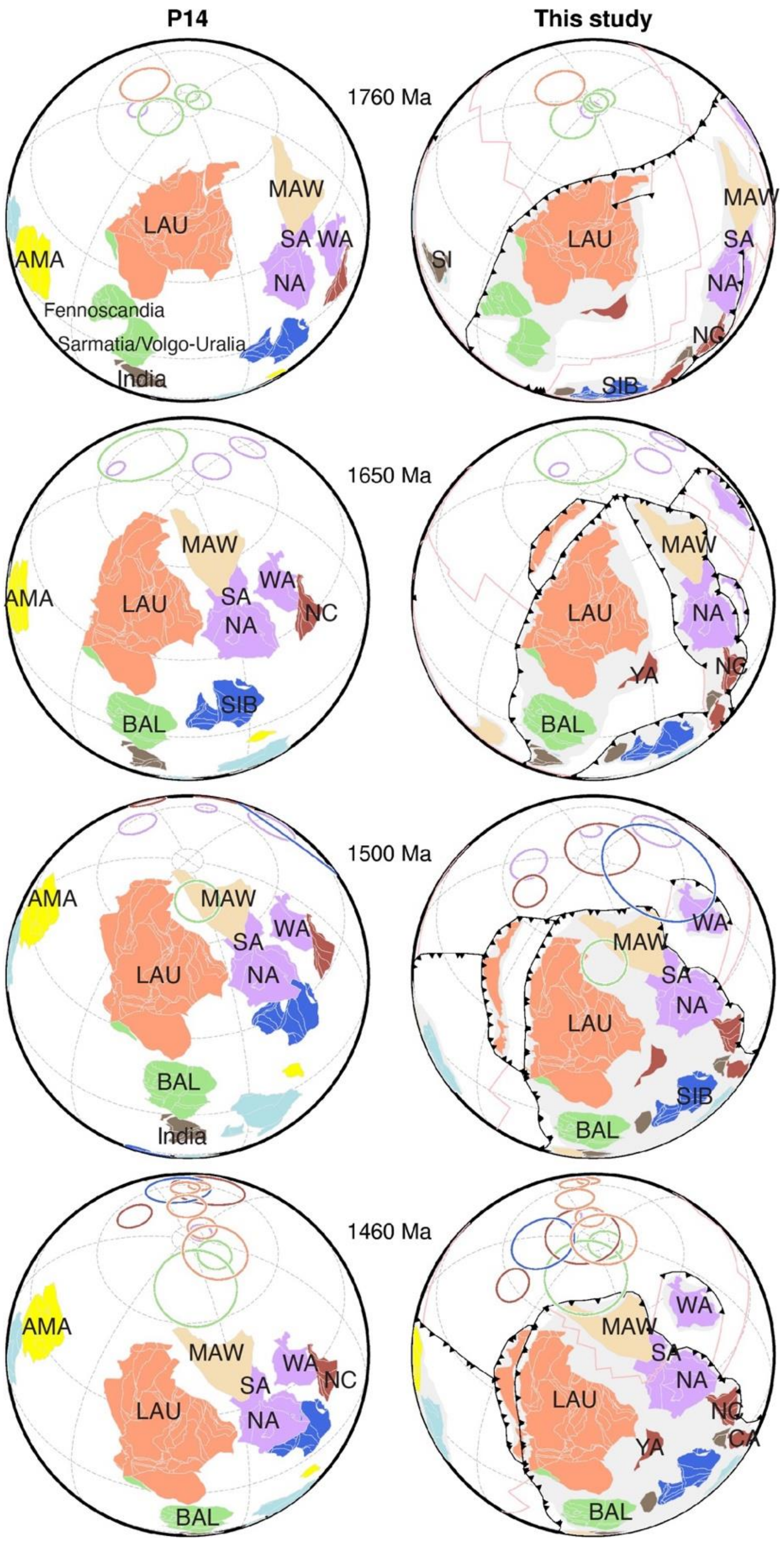

Fig. 6. Evolution of Laurentia and surrounding blocks during Nuna assembly in P14 and in this study. The plate positions are adjusted to better align with

paleomagnetic data. Poles and continents with the same plate ID are shown with the same colours. See Figure 1 for abbreviations.

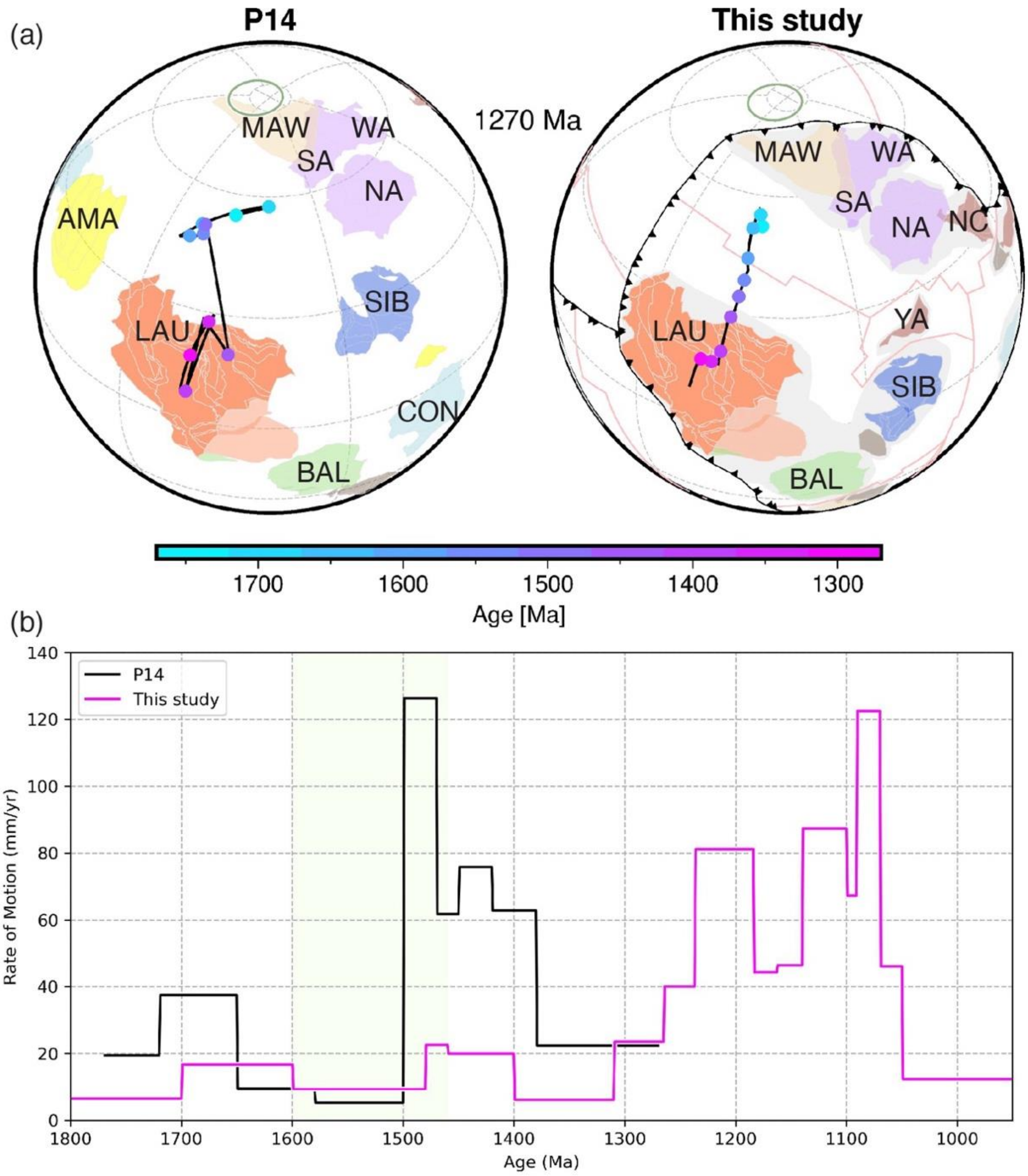

Fig. 7. (a) Motion path and (b) rate of motion of Laurentia in P14 and in this study. The motion of Laurentia is smoother and slower in this study compared with P14. See Figure 1 for abbreviations.

In model P14, southern India is juxtaposed with south-eastern Baltica within Nuna (Fig. 5). This connection is supported by a paleomagnetic pole from the South Indian Block (the ~1466 Ma Lakhna dyke pole; No. 9408 in Table S1), and based on the interpretation that the (present-day) southeastern India margin formed a Paleoproterozoic to Mesoproterozoic active margin in a similar manner to the (present-day) western Baltica margin (Dasgupta et al., 2013). The Indian Archean–Paleoproterozoic basement includes the South and North Indian Blocks that are separated by the Central Indian Tectonic Zone. The amalgamation of the two blocks was previously thought to have occurred during the Paleoproterozoic (e.g. Acharyya, 2003). Three metamorphic-magmatic events occurred along the Central Indian Tectonic Zone: a ca. 1.8–1.75 Ga event in the northern part, and two later events respectively at ca. 1.62–1.54 Ga and ca. 1.06–0.94 Ga in the southern part (Bhowmik and Santosh, 2019; Chattopadhyay et al., 2020; Wang et al., 2021). The ca. 1.06–0.94 Ga event developed considerable crustal shortening and high-pressure metamorphism and is interpreted to mark the final collision between the North and South Indian blocks (Bhowmik and Santosh, 2019; Bhowmik et al., 2012). Therefore, we show the North and South Indian blocks as being separated before this time. Our model considers the juxtaposition of only the South Indian Block with Baltica, as supported by paleomagnetic data, excluding the North Indian Block (Fig. 5).

The southern Eastern Ghats Belt adjacent to the eastern Dharwar Craton of the South Indian Block records ca. 1.90–1.60 Ga accretionary orogenesis, demonstrated by ultra-high temperature (UHT) metamorphism at ca. 1.76 Ga, the formation of magmatic arc at ca. 1.72–1.63 Ga, and subsequent collisional metamorphism at ca. 1.6 Ga (Dasgupta et al., 2013; Henderson et al., 2014). The Napier Complex of East Antarctica is interpreted as colliding with the Dharwar Craton at ~1.60 Ga (e.g. Harley, 2003; Henderson et al., 2014). In M21, the East Antarctic Rayner Province forms an along-strike extension of the northern Eastern Ghats Belt (Eastern Ghats Orogeny) at 1000 Ma, based on similar tectonic and metamorphic histories (Dobmeier and Raith, 2003; Rickers et al., 2001).

The Yangtze Block (western South China) lacks Paleo–Mesoproterozoic paleomagnetic data and is not included in P14. We model the Yangtze Block largely based on a recent geological study (Cawood et al., 2020). Cawood et al. (2020) proposed that the Hainan Island, now a part of Cathaysia Block (eastern South China), was a part of Yangtze Block during Proterozoic times, consistent with a similarities in depositional ages and detrital zircon age spectra as well as Hf isotopic compositions of late Mesoproterozoic sedimentary units from southern Yangtze Block (Kunyang Group) and Hainan Island (Shilu Group) (Wang et al., 2012; Yao et al., 2017). Cawood et al. (2020) suggested that the Yangtze Block was situated offshore northern Laurentia, near northern Australia and southern Siberia in Nuna. This argument is supported by: (1) similar Archean–Paleoproterozoic tectonothermal histories for the Yangtze Block and NW Laurentia. Both regions underwent collision-related regional metamorphism around 2 Ga and subsequent extension-related A-type magmatism and metamorphism at ca. 1.85–1.80 Ga (Cawood et al., 2020; Thorkelson et al., 2001; Wang et al., 2016). (2) The detrital zircon signatures of Late Paleoproterozoic–Mesoproterozoic sedimentary rocks in the Yangtze Block exhibit strong similarities with those from northwest Laurentia and northern Australia. For instance, the detrital zircon age distribution pattern of the late Paleoproterozoic upper Dongchuan Formation matches well with the similar-aged Wernecke Supergroup in northwest Laurentia, the McArthur, Isa, and upper Etheridge successions in North Australia, and the Changcheng Group in North China (Furlanetto et al., 2016; Wang and Zhou, 2014). Similarly, the metasedimentary units in the Baoban Complex in Hainan (part of the Yangtze Block), with ages ranging from 1550 to 1300 Ma, have similar detrital zircon age peaks with time equivalent units in western Laurentia (e.g. Belt Basin), northern Australia (Nordsvan et al., 2018; Yang et al., 2020). (3) The occurrence of similar Fe-Cu mineralization at ca. 1.6 Ga in southwestern Yangtze, northeast Australia, and northwest Laurentia (Thorkelson et al., 2001; Wang and Zhou, 2014). Recently Zhao et al. (2023) proposed that the distinct basement ages between the northern and southwestern Yangtze are comparable to those of southern Siberia and northern Laurentia, respectively. Here we model the Yangtze Block as between northern Laurentia and southern Siberia prior to Nuna breakup (Fig. 6).

3.1.2 East Nuna (Australia, East Antarctica, North China, North India, Cathaysia)

The modern Australian continent consists of three Archean to Paleoproterozoic blocks – the North Australian, West Australian and South Australian cratons. We follow P14 to keep proximity between North and South Australian cratons from 1.8 Ga (see Morrissey et al., 2023 for a recent review). The North Australian Craton underwent a southward motion by ~20° from 1800 Ma to 1760 Ma, as indicated by paleomagnetic data. The southern margin of the North Australian Craton formed a broad accretionary orogen from 1800 to 1500 Ma, which is indicated in the model by the accretion of the Arunta Block at ca. 1740 Ma (representing most of the Aileron Province, Ahmad et al., 2013) and the Musgrave Block at ca. 1600 Ma (which consists of the Warumpi and Musgrave Provinces, Ahmad and Munson, 2013). The accretionary history is manifested by multiple orogenic events (e.g. the 1740–1690 Ma Strangways Orogeny, the 1640–1630 Ma Liebig Orogeny, and the 1600–1560 Ma Chewings Orogeny; Betts et al., 2011; Cawood and Korsch, 2008; Haines et al., 2016). In P14, the West

Australian Craton was fixed to the North Australian Craton before Nuna assembly (Fig. 8). Instead, we model the West Australian Craton to be located near the Kalahari Craton at 1800 Ma. We suggest this proximity to reflect the shared history of the Pilbara and Kaapval cratons (i.e. Vaalbara, de Kock et al., 2009) until ca. 2.1 Ga, followed by the collision between the Pilbara and Yilgarn cratons to form the West Australian Craton represented by the 2005–1950 Ma Glenburgh Orogeny (Johnson et al., 2011; Occhipinti et al., 2004). The West Australian Craton drifted across an ocean (Fig. 8) and collided with the South Australian Craton at ca. 1380 Ma, resulting in the Albany-Fraser (Morrissey et al., 2017; Spaggiari et al., 2018), the Mount West (Howard et al., 2015) and the Parnngurr orogenies (Gardiner et al., 2018; Zhao et al., 2022).

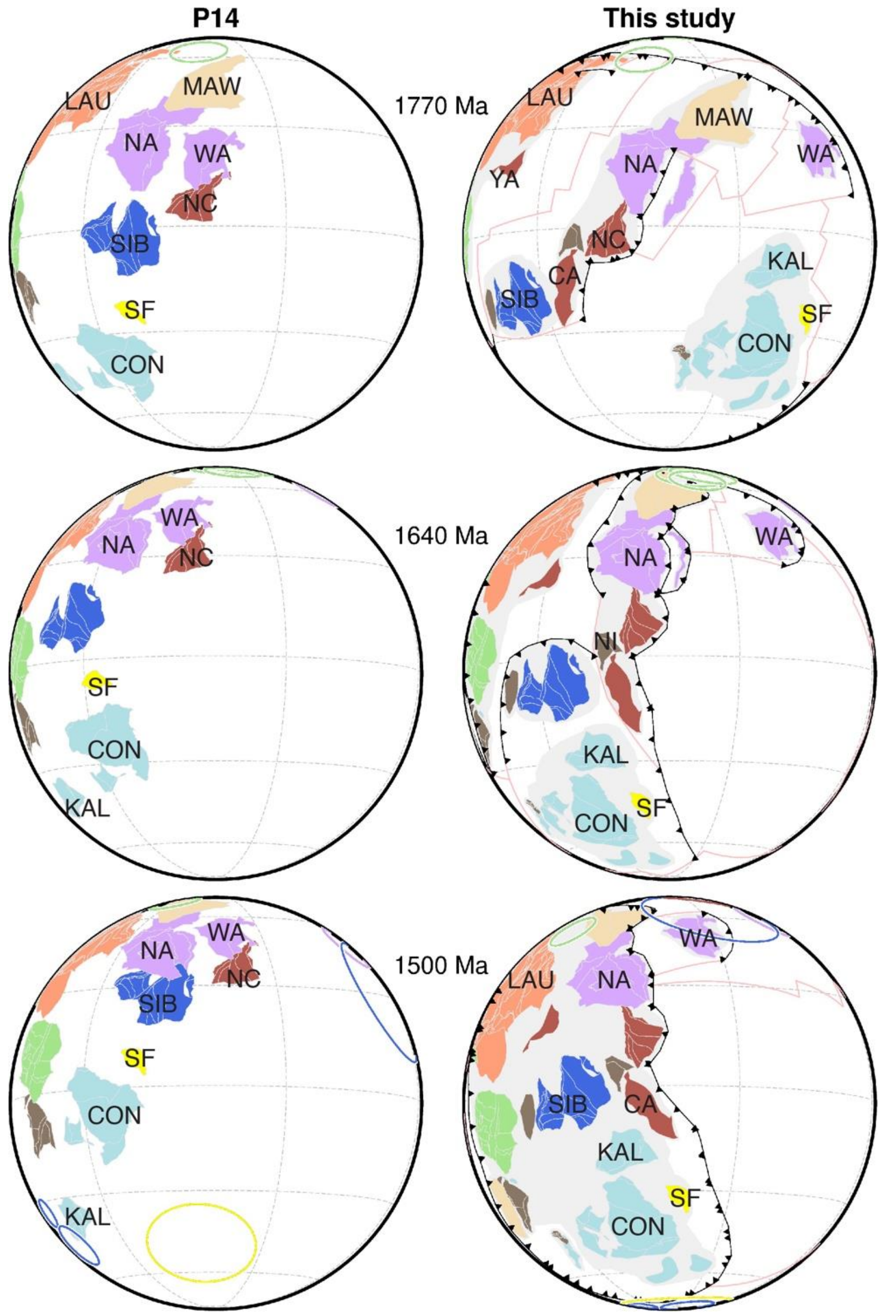

Fig. 8. Evolution of East Nuna in P14 and in this study. The plate configurations are adjusted to better align with paleomagnetic and geological data. Poles and continents with the same plate ID are shown with the same colours. See Figure 1 for abbreviations.

We follow P14 in matching the western Laurentia margin with the northeastern North Australia margin and the eastern South Australia margin (Figs 5, 6 and 8). This interpretation is based on paleomagnetic data and suggestions that eastern Australia-Antarctica provide 1600–1500 Ma zircon detritus for the lower Belt-Purcell Groups and correlatives (Goodge et al., 2017; Ross et al., 1992). We apply a slightly looser configuration than P14, considering that the blocks were likely larger than preserved. The collision between Australia–Antarctica and Laurentia, known as the Racklan orogeny in Laurentia and the Isan Orogeny in Australia, has been recently constrained to ca. 1600 Ma based on geochronological studies (Nordsvan et al., 2018; Pourteau et al., 2018). Therefore, we update the collision time from 1650 Ma in P14 to 1600 Ma. The subduction polarity of the Australia-Laurentia convergence is controversial. The Wernicke Supergroup on the northern part of the western Laurentian margin exhibits a thickness that gradually increases towards the west, indicating a possible passive continental margin prior to the Racklan orogeny (Mitchelmore and Cook, 1994; Thorkelson et al., 2005), even though it was also interpreted as a back arc rifting margin (Nordsvan et al., 2018). The sedimentation age of the Wernicke Supergroup is debated, with studies proposing sedimentation before 1720 Ma (Thorkelson et al., 2005), or until later than 1640 Ma (Furlanetto et al., 2013). To the south of the Mackenzie Mountains, the Muskwa assemblage consists of unmetamorphosed siliciclastic and carbonate strata younger than ca. 1766 Ma based on the youngest detrital zircon (Ross et al., 2001). Seismic studies of these strata suggested a passive margin fabric (Cook et al., 2004). West dipping crust-penetrating thrusts in northeastern Australia (Korsch et al., 2012) fit the metamorphic record suggesting high-pressure ca. 1600 Ma metamorphism in the east forming a lower orogenic plate with the Mount Isa inlier forming an upper plate (Pourteau et al. 2018) whose sedimentary protoliths broadly correlate with coeval sedimentary rocks in the McArthur Basin (overlying the Northern Australian Craton) and are interpreted to be deposited within a basin to the continent side of a subduction zone (Betts et al., 2016; Nordsvan et al., 2018; Rawlings, 1999). Therefore, we model subduction dipping towards Australia.

P14 suggests a close proximity between North China and Australian blocks in Nuna, mainly based on 1.78–1.76 Ga and 1.46–1.41 Ga paleopoles from the two continents (Zhang et al., 2012). The similarity of Mesoproterozoic deposits (Cox et al., 2022), and presence of ca. 1320 Ma LIPs in both northern North China and the McArthur Basin of northern Australia support their proximity (Nixon et al., 2022; Zhang et al., 2012; Zhang et al., 2017). Recent paleomagnetic data also support the long-lived (~1.78 to 1.32 Ga) connection between North China and North Australia (Wang et al., 2019). We maintain the North China-Australia connection but with slight adjustments. Instead of locating North China adjacent to the southwestern (present-day) North Australia, we position it next to the western margin, with subduction along the southern margin of North Australia (Fig. 8). The connection between North China and Australia is maintained during the period of 1000–650 Ma in model M21. Thus, we keep the two blocks next to each other from 1800 Ma and 650 Ma, and apply a small shift between them between 1236–1200 Ma to achieve a better fit with the paleomagnetic data. Overall, our updated configuration improves the match with paleomagnetic data (Fig. S1) and simplifies the transition to the Rodinia configuration. The Mesoproterozoic Xiong'er Group in the southern North China Block consists of andesites and basaltic andesites formed at 1.78–1.75 Ga (He et al., 2009), with minor felsic volcanic rocks erupting at ca. 1.45 Ga, with lithological characteristics suggesting long-term subduction along the southern margin (Chen, 1992; Chen and Zhao, 1997; Zhao et al., 2003b). During this period, the northern margin of the North China Block experienced muti-stage intracontinental rifting (e.g. the Yanliao rift), and the deposition of thick clastic rocks and limestone between ca. 1.7–1.4 Ga (Li et al., 2019).

The North Indian and South Indian blocks were recently suggested to have been separate in the Mesoproterozoic until amalgamation at ~1.0 Ga (see above). Based on similarities in Archean–Proterozoic metamorphic evolution, orogenesis and sedimentary-volcanic successions, North China and India were proposed to have been connected in Nuna, with the East and West blocks of North China connected to the South and North Indian blocks, respectively (Zhao et al., 2002). This configuration is adopted by many studies (Li et al., 2019; Zhang et al., 2012). Pisarevsky et al. (2013) argued that a ca. 1466 Ma paleomagnetic pole from South India ruled out its position close to North China, and suggested a position next to Baltica. The location of North India is unconstrained. Here we tentatively leave the North Indian Block next to the western North China prior to Nuna breakup, and attach its northwest margin to the northern margin of North China (similar to Fig.4 of Wang et al., 2021). As with many of the links proposed here, this positioning may need refinement as additional data becomes available.

The Cathaysia Block (eastern South China) is not included in P14 due to a lack of paleomagnetic data. Previous interpretations suggested a connection between Cathaysia and Southwest Laurentia in the Paleo-Mesoproterozoic, based on similarities between the 1430 Ma granites on Hainan Island (southwestern Cathyasia block) and similar-aged A-type granite province of Southwest Laurentia (Li et al., 2008; Yao et al., 2017). However, recent studies indicate that the Precambrian crustal components of Hainan Island are unrelated to Cathaysia but are instead linked to the Yangtze Block (Cawood et al., 2020; Wang et al., 2021; Xu et al., 2016). Recent proposals suggest a connection between the Cathaysia Block and the Lesser

Himalaya of North India during the Proterozoic (Cawood et al., 2020; Wang et al., 2021), which is also adopted in model M21 for the Rodinia interval. High-grade metamorphism at 1.88–1.86 Ga in both the Cathaysia Block and Lesser Himalayan Block has been proposed to mark their collision (Richards et al., 2005; Yu et al., 2012). The collision was followed by synchronous (~1.83–1.80 Ga), within plate, mafic volcanism in the Aravalli-Delhi Fold Belt and Lesser Himalaya of the North India Block, and the Cathaysia Block (Liu et al., 2014; Miller et al., 2000; Wang et al., 2021). In addition, Paleoproterozoic sedimentary successions from both the North India Block (e.g. the Aravalli and Northern Delhi Supergroups; Long et al., 2011; McQuarrie et al., 2008) and Cathaysia Block (e.g. the Badu Complex; Yu et al., 2012) exhibit similar detrital zircon age peaks at ~2.5 Ga and ~1.85 Ga (Cawood et al., 2020; Wang et al., 2021). Therefore, we locate the Cathaysia Block adjacent to northern North Indian Block during the late Paleoproterozoic to Mesoproterozoic eras (Fig. 8).

3.1.3 South Nuna (Siberia, Tarim, Congo/São Francisco, Kalahari)

Siberia, which is nearly surrounded by Mesoproterozoic passive margins, is generally located in the interior of Nuna (Evans and Mitchell, 2011; Pisarevsky and Natapov, 2003). Many previous studies suggest Siberia existed off the northern Laurentia margin in Nuna, although different configurations have been proposed (Ernst et al., 2016; Pisarevsky et al., 2014; Zhao et al., 2002). Based on paleomagnetic data, P14 and related earlier studies (e.g. Pisarevsky et al., 2008) proposed that Siberia was located near the present-day northwest of Laurentia with a big ‘gap’ between 1500 and 950 Ma. We accept the ‘gap’ proposal, but with adjustments to better match paleomagnetic poles (Fig. S1). The fit of two poles from southeast Siberia at 1730–1720 Ma (poles No. 9500 and 9501 in Table S1) with a ~1745–1736 Ma pole from Laurentia (pole No. 9139 in Table S1) indicates a greater distance compared to those of 1475 Ma and 1050–950 Ma, suggesting that Siberia joined Laurentia-Baltica between 1740 Ma and 1475 Ma. Following recent suggestions of Cawood et al. (2020, Pisarevsky et al. (2021) and Zhao et al. (2023) we tentatively model Siberia accreting onto West Nuna at 1600 Ma with Yangtze placed between southern Siberia and northern Laurentia (Fig. 8).

Tarim was not included in P14 and most previous models due to limited geological studies and a lack of paleomagnetic data. Recent research on the northern Tarim margin has revealed a 1.94–1.91 Ga magmatic-metamorphic event occurred in an Andean-type continental arc, which was followed by collision at ca. 1.9–1.8 Ga (Ge et al., 2015). Similarly, collision-related granitic rocks of 2.0–1.8 Ga age are found in southern Siberia (Wang et al., 2020). Detrital zircons from Proterozoic strata of northern Tarim and southern Siberia show a peak at 2.0–1.8 Ga and a lack of zircons between 1.7–1.1 Ga. Moreover, 2.0–1.8 Ga detrital zircons from the two continents show remarkably similar εHf(t) values. Consequently, Wang et al. (2020) proposed that Tarim-Siberia were juxtaposed in Nuna after collision at 2.0–1.8 Ga. The Tarim-Siberia configuration is adopted in our model (Fig. 5).

In P14, the Congo/São Francisco craton is positioned directly south of Siberia, with São Francisco connected to the northern Siberia margin. Due to the lack of high quality paleomagnetic poles, this argument is mainly based on coeval ca. 1500 Ma dyke swarms and ca. 1380 Ma magmatic events (Ernst et al., 2013). Here, based on ca. 1500 Ma palaeomagnetic poles from the two continents (poles No. 9552 and 9558), the Congo/São Francisco craton is rotated clockwise by 80° relative to Siberia compared to the P14 configuration, with southern Congo facing northern Siberia, and also a larger distance between the two blocks (Fig. 5). At around 1790 Ma, we position the Congo/São Francisco craton to the east in the open ocean, with its latitude constrained by a paleomagnetic pole. We then employ a westward motion of the craton (Fig. 8), leading to its eventual joining with Siberia at 1650 Ma.

There are no reliable paleomagnetic data to constrain the location of Kalahari in Nuna. In P14, Kalahari forms the southernmost part of Nuna, surrounded by oceans, following Pesonen et al. (2003) and Jacobs et al. (2008). Recent studies suggest that dykes dated at ca. 1110 Ma in southern Congo may represent radial arms of the coeval Umkondo LIP in northern Kalahari as they have similar compositions, suggesting a possible connection between the two continents (de Kock et al., 2014; Ernst et al., 2013). Moreover, based on new paleomagnetic poles from the Kalahari dykes and the Umkondo LIP, Salminen et al. (2018) proposed a Kalahari-Congo configuration at 1110 Ma that is slightly different from that of the present-day. In this study, we adopt the Kalahari-Congo configuration proposed by Salminen et al. (2018) and extend it back to 1.8 Ga (Fig. 5).

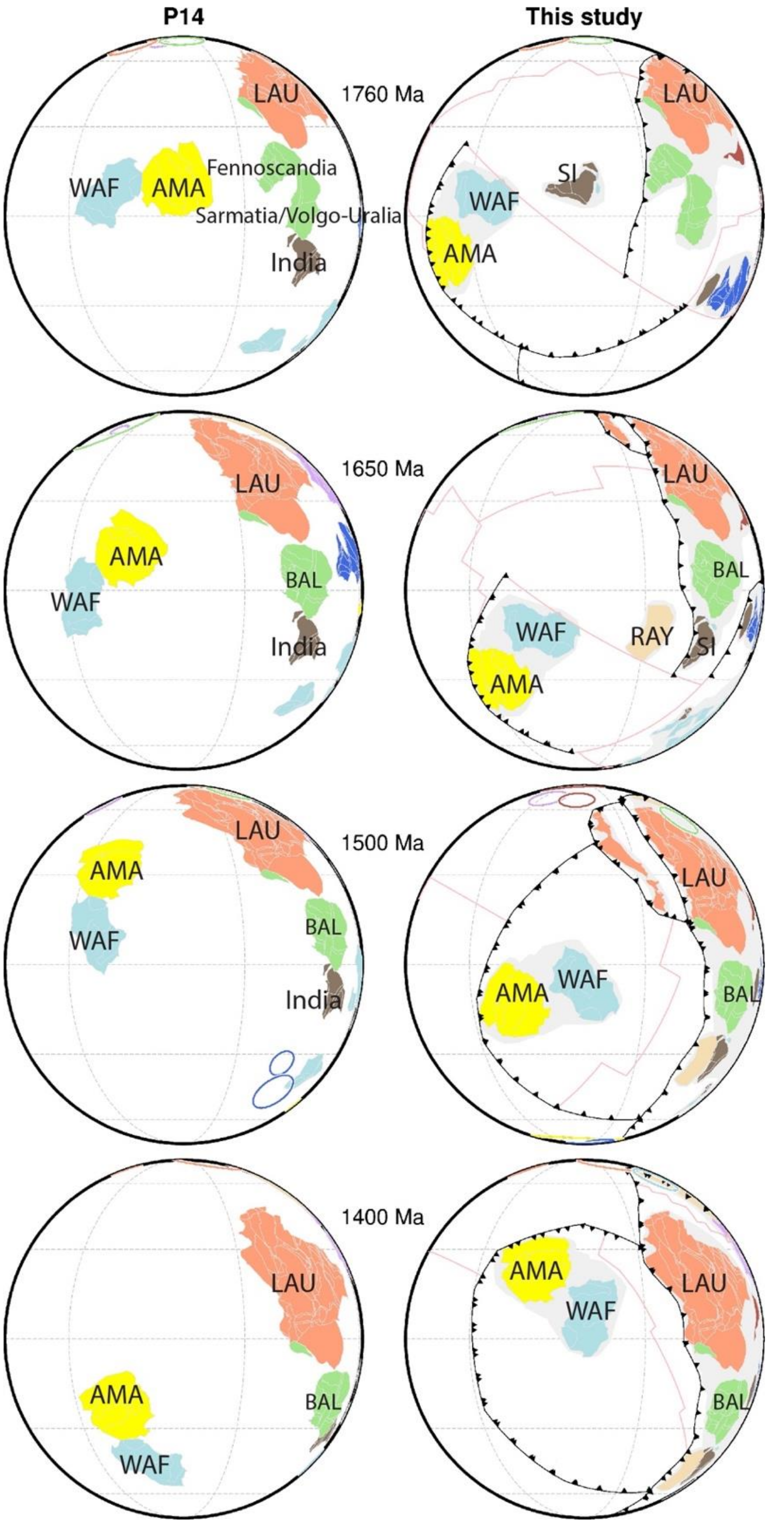

Fig. 9. Tectonic evolution of Amazonia-West Africa in P14 and in this study. The two blocks are inferred to be located within a large ocean basin, distal to other continents from 1.8 Ga to 1.0 Ga. Their paleolatitude is constrained by paleomagnetic data. See Figure 1 for abbreviations.

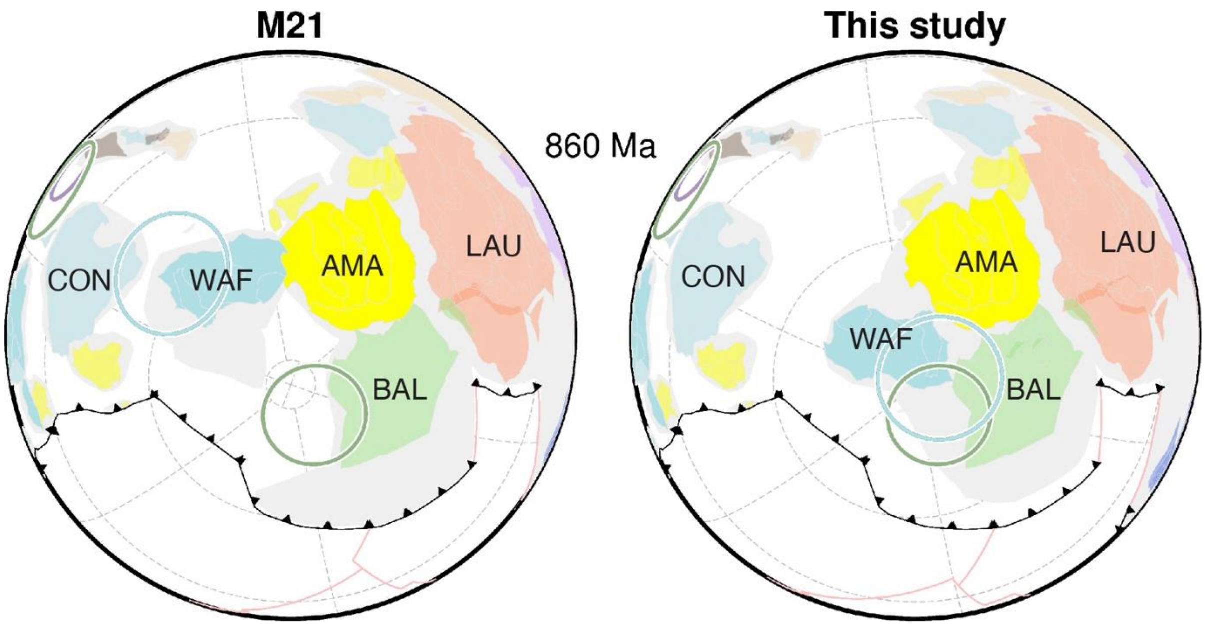

Fig. 10. West Africa-Amazonia configuration in Merdith et al. (2021, left) and in this study (right). West Africa is rotated relative to Amazonia based on a pole (the light blue circle, pole No. 9968; Antonio et al., 2021) at 860 Ma. Poles and continents with the same plate ID are shown with the same colours. See Figure 1 for abbreviations.

3.1.4 Amazonia and West Africa

We leave West Africa-Amazonia separate from Nuna following P14 (Fig. 9). The hypothesis of Trompette (1994) that West Africa and Amazonia constituted a rigid continent resembling their Gondwanan configuration since the Mesoproterozoic has been widely accepted (e.g. Evans and Mitchell, 2011; Zhang et al., 2012). However, to match a recently published pole (No. 9968 in Table S1) from West Africa at 860 Ma (Antonio et al., 2021), maintaining the Gondwanan configuration for the two blocks in Rodinia would require an anticlockwise rotation for them by ~80° relative to Laurentia, which is unreasonable. Here we keep the well-constrained Amazonia-Laurentia configuration in Rodinia, but introduce a new configuration for the Amazonia and West Africa based on the 860 Ma pole (Fig. 10). Other updates to P14 include: (1) making the southwestern margin of Amazonia, where subduction occurs, face the superocean most of the time (Fig. 9), and (2) applying four new poles. In our model, the Amazonia and West Africa continental blocks drifted in the ocean ~2000–5000 km west of Laurentia-Baltica from 1800 Ma until the assembly of Rodinia. We anticipate that this simple configuration will be improved as more data become available.

3.2. Nuna breakup and the initial assembly of Rodinia (1460–1000 Ma)

The breakup process of Nuna is not well described in the base models, as P14 ends at 1270 Ma, and C21 ends at 1100 Ma with ~100 Myr temporal resolution. For the period before 1100 Ma, we refine the base models using available paleomagnetic poles and geological observations. For the 1100–1000 Ma period, we model the plates to obtain a smooth transition to M21.

During the late Mesoproterozoic, Baltica underwent a significant clockwise rotation by ~95° relative to Laurentia (Cawood et al., 2010). The exact timing of this rotation is uncertain. In C21, the separation between Baltica and Laurentia is modelled as beginning between 1300 Ma and 1200 Ma. Paleomagnetic data suggest that the clockwise rotation started after 1270 Ma and finished between 1050 Ma and 1000 Ma (Pisarevsky and Bylund, 2010; Pisarevsky et al., 2003; Salminen and Pesonen, 2007), coinciding with the collisional stages of the Grenville-Sveconorwegian orogeny (Bingen et al., 2008). Some studies propose that the clockwise rotation occurred between 1120 Ma and 1050 Ma (Evans, 2009; Salminen et al., 2009). This breakup is also proposed to be related to the 1270 Ma giant McKenzie magmatic event (Park, 1992) and the similar-aged Central Scandinavian Dolerite Complex (Elming and Mattsson, 2001). Structural evidence from Starmer (1996) suggests that the separation started around 1240 Ma. Considering these large uncertainties, we model the clockwise rotation occurring between 1235 Ma and 1020 Ma.

The timing of the breakup between South India and Baltica is poorly constrained, because there is no evidence of Mesoproterozoic rifting in the western Dharwar Craton or the southwestern margin of Sarmatia (Pisarevsky et al., 2014). The breakup is not included in model P14 and starts between 1300 Ma and 1200 Ma in C21. But P14 suggested a possible relation between the 1300–1100 Ma mafic sills in the western part of the Volyn-Orsha aulacogen (Bogdanova et al., 2008) and the Baltica-India rifting. They also proposed that the 1300–1100 Ma Volyn-Orsha aulacogen may represent a failed arm of a triple junction (Bogdanova et al., 1996) during the Baltica-India rifting. Additionally, a ca. 1190 Ma pole indicates South India was located at high latitudes, while Greenland (indicated by 1189–1179 Ma poles) and Baltica were at low latitudes, suggesting an earlier breakup timing. A breakup timing of 1270 Ma is adopted here.

The separation between Australia-Mawson and Laurentia is included in P14, which is largely adopted here (Fig. 11). According to P14, South Australia-Mawson rifted from Laurentia at ca. 1460 Ma, followed by the separation of North Australia at ca. 1380 Ma. This rift event marks the onset of Nuna breakup, which could be associated with the 1.38 Ga Hart River magmatism in northwest Laurentia, and subsequent deposition of the Pinguicula Group (Medig et al., 2009). This interpretation also agrees with a new ca. 1320 Ma pole from North Australia (pole No. 9978 in Table S1)(Kirscher et al., 2021), which indicates that Australia was not far from Laurentia at this time. The sedimentary/provenance record of northern Australia (Yang et al., 2023; Yang et al., 2020) is interpreted to match the magmatic record of rifting in northern South Australia (Morrissey et al., 2019) to reflect a relatively early (ca. 1450 Ma) rifting between Australia and Laurentia. In model M21, dextral motion between Australia-Mawson and Laurentia during the late Stenian to early Tonian is proposed until the assembly of Rodinia, following Mulder et al. (2018). We adopt this dextral motion model but locate Australia-Mawson a little further away from Laurentia at 1070 Ma, to slightly improve agreement with paleomagnetic data. In summary, in our model Australia-Mawson rifts from Laurentia at 1460–1380 Ma, with spreading in the intervening ocean terminating at 1200 Ma. This episode of spreading is followed by a period of sinistral motion until 1070 Ma, followed by a resumption of dextral motion until the final assembly of Rodinia at 930 Ma, consistent with M21 and with paleomagnetic data. In our model, the North China and Australian blocks remain juxtaposed during the Nuna breakup process. In addition, we also model South China to begin rifting from Laurentia at 1380 Ma.

P14 proposed that Siberia could stay fixed to Laurentia with a gap (filled by Yangtze in our model) between them between 1500 Ma and 950 Ma base on paleomagnetic poles. Even though the long-term relatively fixed Siberia and Laurentia configuration is feasible, we impose a small amount of rifting between the Siberia-Tarim and Laurentia-Baltica from 1235 Ma to 1200 Ma to achieve a better match with paleomagnetic poles during 1100–1000 Ma and 1500–1450 Ma. The onset of the rifting is modeled to occur simultaneously with the separation of Baltica from Laurentia, forming a triple junction between Siberia, Baltica and Laurentia (Fig. 11).

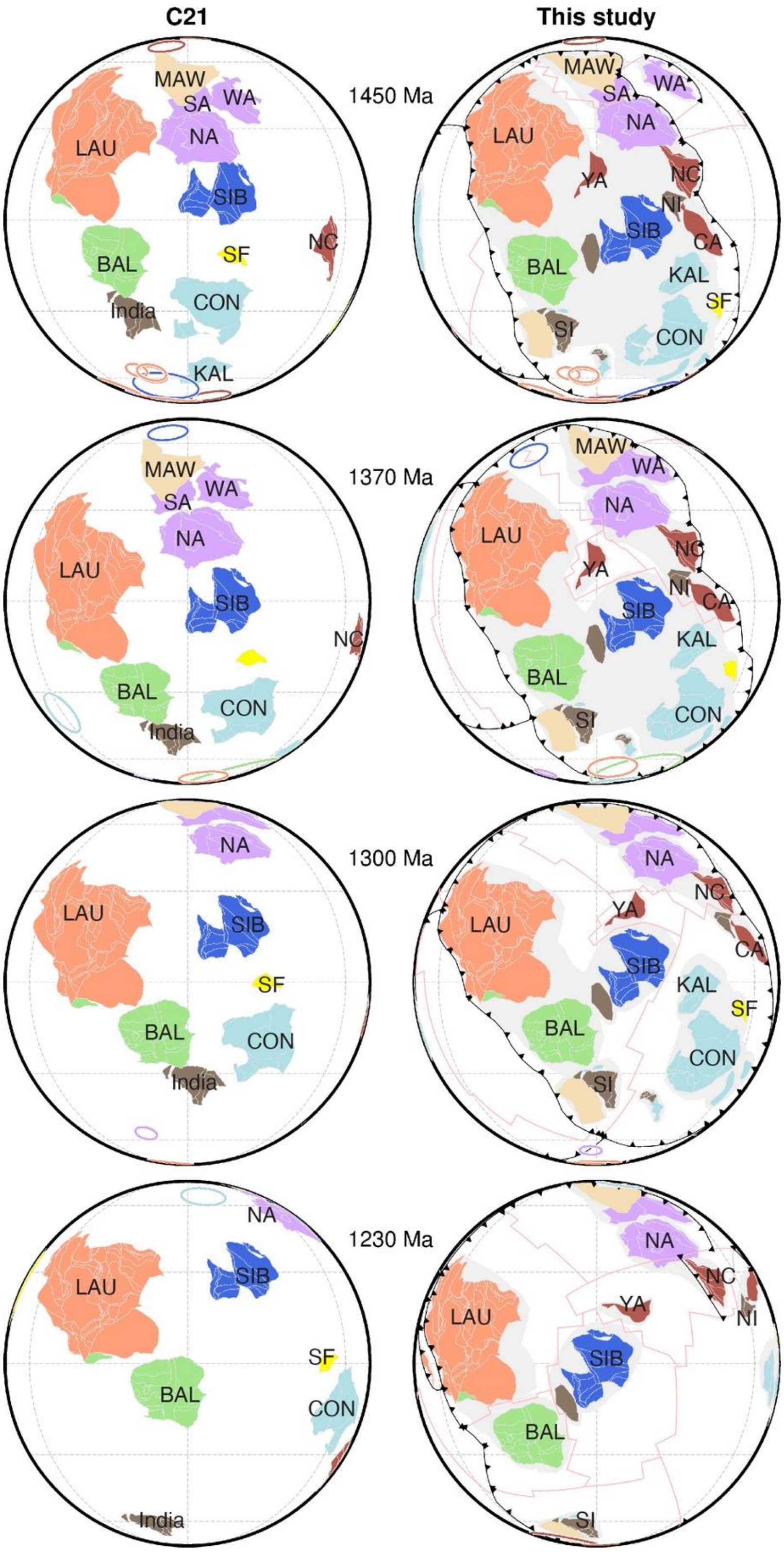

Fig. 11. Comparison of the breakup of Nuna in C21 and in this study. The breakup initiates at 1.46 Ga from the north and progresses southward in our model. The rift history of the Australian blocks is largely adopted from P14 and C21, while other

blocks are significantly refined or new modelled using available data. See Figure 1 for abbreviations.

A ca. 1236 Ma paleomagnetic pole (pole No. 8123, Meert et al., 1994) indicates a significant distance between Congo/São Francisco and Laurentia at that time, suggesting an earlier breakup. We model the breakaway time of Congo/São Francisco at 1300 Ma, which aligns with the timeframe modelled in C21 (between 1300 and 1200 Ma). During Nuna breakup, Kalahari remained attached to Congo/São Francisco, as supported by poles at ca. 1110 Ma (Salminen et al., 2018; Swanson-Hysell et al., 2015). They are separated in Rodinia (as in M21), with Congo/São Francisco at high latitude at ca. 900 Ma, and Kalahari at low latitude (Evans, 2013). The emplacement of the ca. 1110 Ga Umkondo LIP likely signifies the breakup of the Congo/São Francisco and Kalahari cratons (Salminen et al., 2018). We model the breakup at 1105 Ma, followed by separate accretions of the two blocks onto Rodinia.

Amazonia is traditionally positioned adjacent to Laurentia in Rodinia, with the 1300–1000 Ma Sunsas orogenic belt of southwest Amazonia (Litherland and Power, 1989; Santos et al., 2000) paired with the Grenville Orogen on the eastern margin of Laurentia (e.g. Hoffman, 1991; Pisarevsky and Natapov, 2003). Previous geological and paleomagnetic studies have suggested that Amazonia collided with the southern Grenville Province, followed by a ~3000 km sinistral strike-slip movement towards Baltica and northern Laurentia between 1200 and 1000 Ma (Tohver et al., 2005a; Tohver et al., 2005b; Tohver et al., 2002). Evans (2013) proposed a clockwise rotation of Amazonia into Laurentia between ca. 1200 Ma and 1000 Ma, using the opposite polarities of the paleomagnetic poles and assuming a Mesoproterozoic Baltica-Amazonia connection. Apart from the poles used in previous studies, a new pole at

1110 Ma (Bispo-Santos et al., 2023) is used here. We consider a clockwise rotation between 1200 Ma and 1110 Ma, followed by an anticlockwise rotation until the final collision at 1000 Ma.

3.3 Rodinia final assembly and post-Rodinia (1000 Ma–present)

We have made minor modifications to M21 based on new data. One important change is to the evolution of West Africa, which underwent rifting from Amazonia during the breakup of Rodinia and subsequently accreted onto the Sahara Metacraton to form the African continent (Fig. 12). This alteration is partly because the West Africa-Amazonia configuration is changed here based on an 860 Ma pole (Fig. 10). We adjust the rift timing from 850 Ma in M21 to 720 Ma in our model based on the observation that rocks of the middle Neoproterozoic Assabet el Hassiane Group (Mauretanian Taoudeni Basin) appear to be deposited within active rift basins (Bradley et al., 2022). We still follow M21 in modelling the accretion onto the Sahara Metacraton at 600 Ma.

In addition, the breakup time between Australia and Laurentia is changed from 800 Ma in M21 to 780 Ma in our model. Geological and paleomagnetic data suggest a poorly constrained rifting and transition from rift-to-drift between Australia and Laurentia between 825 and 700 Ma (e.g. Merdith et al., 2017a). While M21 adopted an early rifting at 800 Ma to achieve a low relative spreading velocity, they acknowledged that a later rifting before 770 Ma is kinematically feasible. Here we update the breakup timing to 780 Ma, to achieve a slightly better fit to a new 775 Ma pole (No. 9975 in Table S1) from North China.

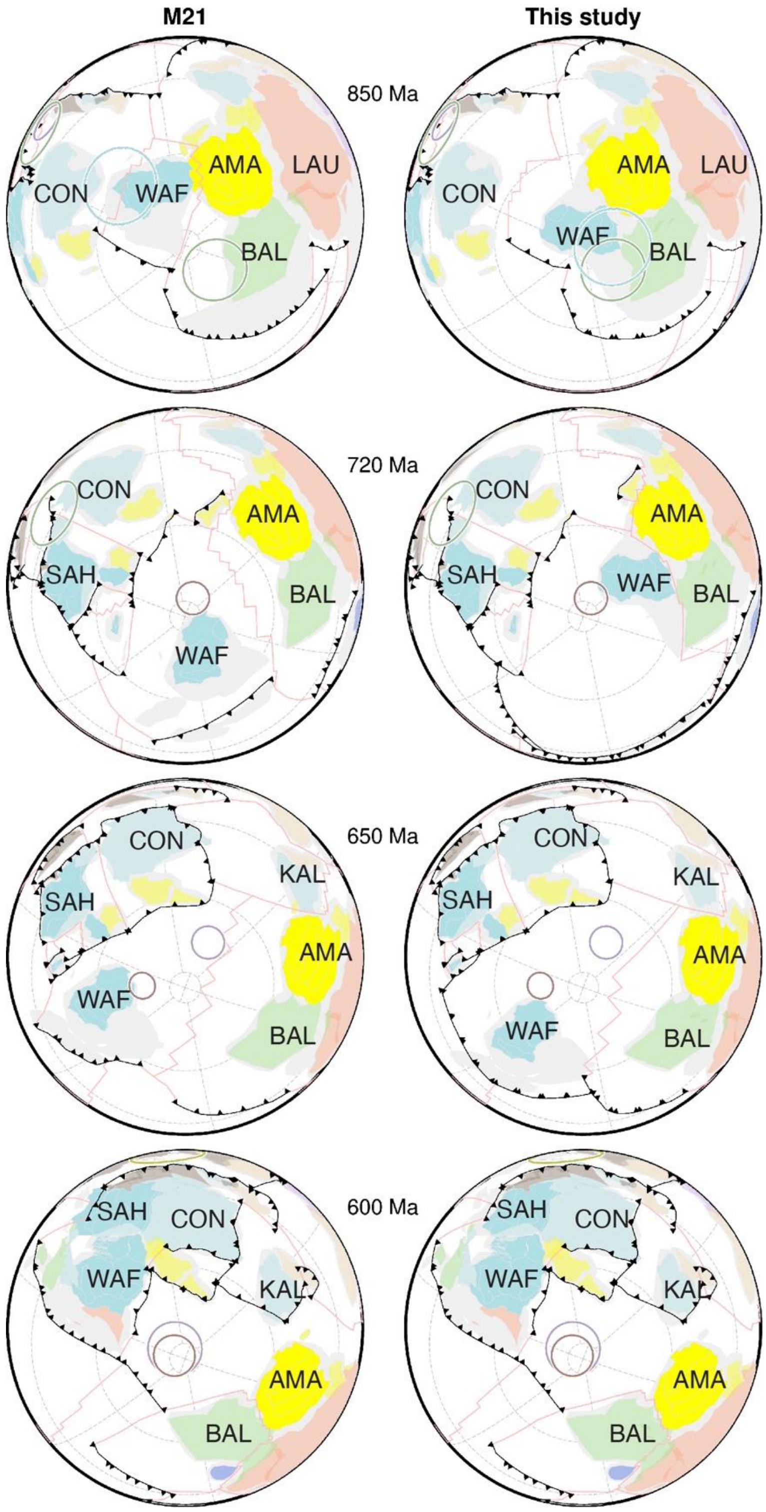

Fig. 12. Breakup of West Africa and Amazonia in M21 (left) and in this study (right). The rift timing of West Africa from Laurentia and Amazonia is adjusted from 850 Ma in M21 to 720 Ma in our model, followed by the accretion onto the Sahara Metacraton at 600 Ma following M21. See Figure 1 for abbreviations.

We make slight adjustments to South China and India to better match an 802 Ma pole from South China (No. 9117 in Table S1). Following M21, we maintain the connection between South China and India during the late Mesoproterozoic and Neoproterozoic eras based on their comparable Tonian accretionary histories. In addition, we have made other very minor alterations including slightly adjusting the relative positions of North China and North Australia to avoid overlap and adjusting the position of Siberia to better matching paleomagnetic data between 1050 Ma and 950 Ma.

4. Global plate model between 1.8 Ga and 1.0 Ga

The base models provide detailed descriptions of the global reconstructions, and our updates to them are outlined in Section 3. In this section, we provide a summary of the major tectonic events occurred between 1.8 Ga and 1.0 Ga, which are the focus of our refinements in this study.

Our model starts with a quasi-supercontinent at 1.8 Ga (Fig. 13), with most continents in geographical proximity at low latitudes. At 1.7 Ga, the collision between Sarmatia/Volgo-Uralia and Fennoscandia resulted in the formation of Baltica. Concurrently, South India joined Baltica and Laurentia, forming the West Nuna continent. To the east, the Australia blocks, Mawson, North China, North India, and Cathaysia formed East Nuna. East and West Nuna were separated by a narrow ocean at 1.8 Ga. Siberia had not joined Laurentia at this point, constrained by a pole at ca. 1.72 Ga. Congo/São Francisco and Kalahari moved westward from the open ocean and joined Siberia at 1.65 Ga to form South Nuna. Eventually, the East, West, and South Nuna merged at 1.6 Ga, causing the Racklan/Isan orogeny (e.g. Pourteau et al., 2018; Volante et al., 2020).

After assembly, Nuna was centred at the equator and exhibited very slow anticlockwise motion before its eventual breakup. This rotation was interpreted as true polar wander by Li et al. (2013). In the opposite hemisphere, the superocean was occupied by three large oceanic plates. Nuna's exterior margin experienced long-term accretionary orogenesis that is found preserved along the margins of eastern Laurentia, southwestern Baltica, eastern Dhawar, southern North China, and southern North Australia (Fig. 4). Note that rather than the proposed Proterozoic stagnant-lid hypothesis of Stern (2018), this extensive subduction/accretion orogenesis reflects Phanerozoic-like plate tectonics in the presence of a major supercontinent.

The breakup of Nuna primarily occurred between ca. 1.46–1.3 Ga, initiating from the north and progressing towards the south. At 1.46 Ma, Mawson and South Australia began to rift away from Nuna. This rifting was followed by the separation of North Australia, Yangtze, North India, and Cathaysia at 1.38 Ga. West Australia collided South Australia and North Australia at 1.38 Ga, suggesting that it was never a part of Nuna. Subsequently, at 1.3 Ga, Congo/São Francisco and Kalahari separated from the supercontinent, with Congo shifting from 30°S to an equatorial region by 1.24 Ga. South India broke away from Baltica at 1.27 Ga and moved towards the polar area. The breakup of Nuna was accompanied by the extensive formation of LIPs throughout the interior of Nuna during 1.4–1.3 Ga (Li et al., 2019; Zhang et al., 2022). Examples include the 1.38 Ga Hart River–Salmon River Arch LIP in western Laurentia (Doughty and Chamberlain, 1996), the 1.38 Ga Midsommersø–Zig-Zag Dal LIP in eastern North Greenland (Upton et al., 2005), the 1.32 Ga Yanliao LIP in North China (Zhang et al., 2017), and the 1.32 Ga Derim Derim-Galiwinku LIP in North Australia (Nixon et al., 2022).

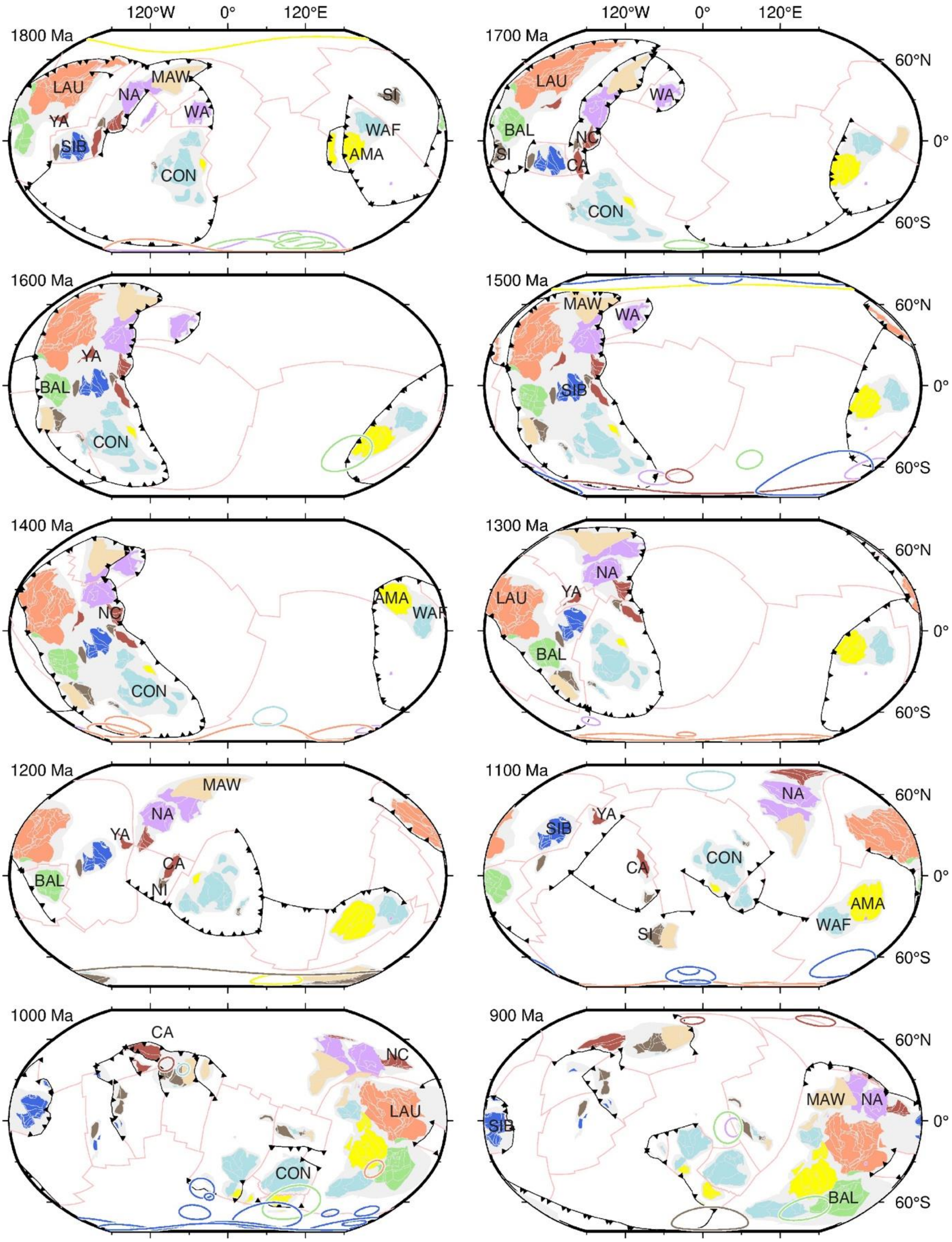

Fig. 13. Global plate reconstructions between 1800 and 900 Ma. The model starts with a quasi-supercontinent at 1.8 Ga. The East, West, and South Nuna merged at 1.6 Ga, causing the Racklan/Isan orogeny. The breakup of Nuna primarily occurred between ca. 1.46-1.3 Ga. After the breakup of Nuna, the continental blocks came back

together at 930 Ma, forming Rodinia. West Africa and Amazonia stayed in the ocean to the west of Nuna from 1800 Ma until their collision with Laurentia at 1000 Ma. See Figure 1 for abbreviations.

Baltica experienced a ~95° clockwise rotation relative to Laurentia between 1235 and 1020 Ma, and remained adjacent to Laurentia in the Rodinia supercontinent (Cawood et al., 2010). Congo/São Francisco and Kalahari moved eastward across the ocean and reached their westernmost position in Rodinia as depicted in M21. We try to model the movement of these blocks along the shortest path. North India and the Cathaysia Block remained connected during the breakup of Nuna and assembly of Rodinia. Around 900 Ma, Yangtze accreted onto Cathaysia to form South China, and at ~980 Ma, South India accreted onto North India to form Neoproterozoic India (Collins and Pisarevsky, 2005). South China and India remained outside of Rodinia following M21. After the breakup of Nuna, the Australian blocks and North China gradually drifted away from Laurentia until 1200 Ma. Subsequently, they underwent left-lateral transform movement relative to Laurentia, followed by right-lateral shear after 1070 Ma. They ultimately rejoined Laurentia at 930 Ma, marking the final formation of Rodinia.

In our model, West Africa and Amazonia stayed in the ocean to the west of Nuna from 1800 Ma until their collision with Laurentia at 1000 Ma. The positions of the two blocks during this period are constrained by nine paleomagnetic poles (one pole from West Africa, and eight from Amazonia).

5. Model analysis and discussion

We quantify and evaluate the model in terms of the match to paleomagnetic data (Fig. 14), the lengths of ridge and trench, and associated plate motion rate through time (Fig. 15). We calculate the misfit between our model and the paleomagnetic poles, which is defined as the minimum great circle distance between the North Pole and the reconstructed paleomagnetic pole within the valid time range (Merdith et al., 2021). The mean misfit for all plates is about 12° (Figs 14 and S1), which is smaller than the 19° misfit for P14. The large misfit of P14 is partly due to the fact that some of the poles were published after the development of that model.

The total length of subduction zones shows consistency for the entire model period. However, the length of mid-ocean ridges and transforms for 1.8–1.0 Ga is considerably shorter than that of present-day (but is not very different from that of the Paleozoic). The short length of ridge is likely because: (1) we only model major cratonic blocks in the Proterozoic, which produce less ridges when continents breakup, and (2) we build simple three-ridge configurations for major oceans, which contrasts with the modern Pacific Ocean, which is characterized by a larger number of plates, and therefore long ridges and transforms. The length of mid-ocean ridges is low during times of supercontinent existence, and high during times of supercontinent break up. For example, mid-ocean ridge length peaks at ca.1200 Ma, 550 Ma and 150 Ma, when Nuna, Rodinia, and Pangea fully break up, respectively. Then the length decreases when the planet enters the assembly stage of the successive supercontinent. We don't see a similar trend in subduction zone length.

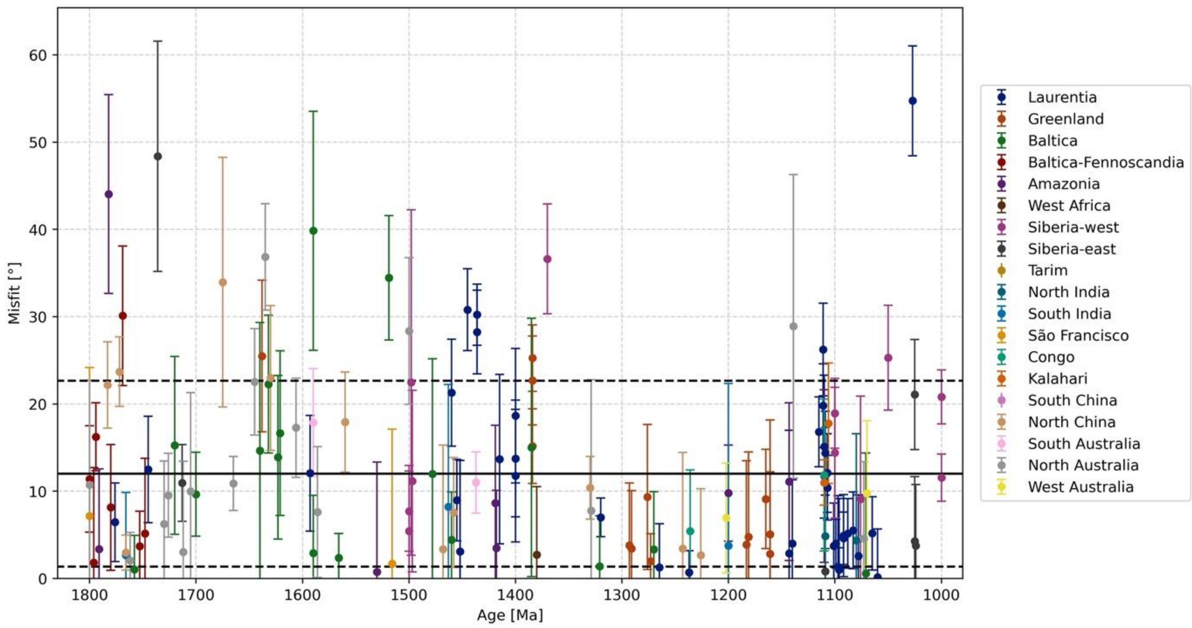

Fig. 14. Fit of palaeomagnetic data to our model. The misfit is defined as the minimum great circle distance between the North Pole and the reconstructed palaeomagnetic pole within the valid time range (Merdith et al., 2021)**.** The misfit between the paleomagnetic poles and our reconstructions are generally below 25°, with a mean of around 12°, which is similar to the misfit in M21 for the last 1 Gyr. The solid line denotes the mean misfit of all poles, and the dashed lines denote the corresponding standard deviation. The error bars denote 95% confidence limits (A95).

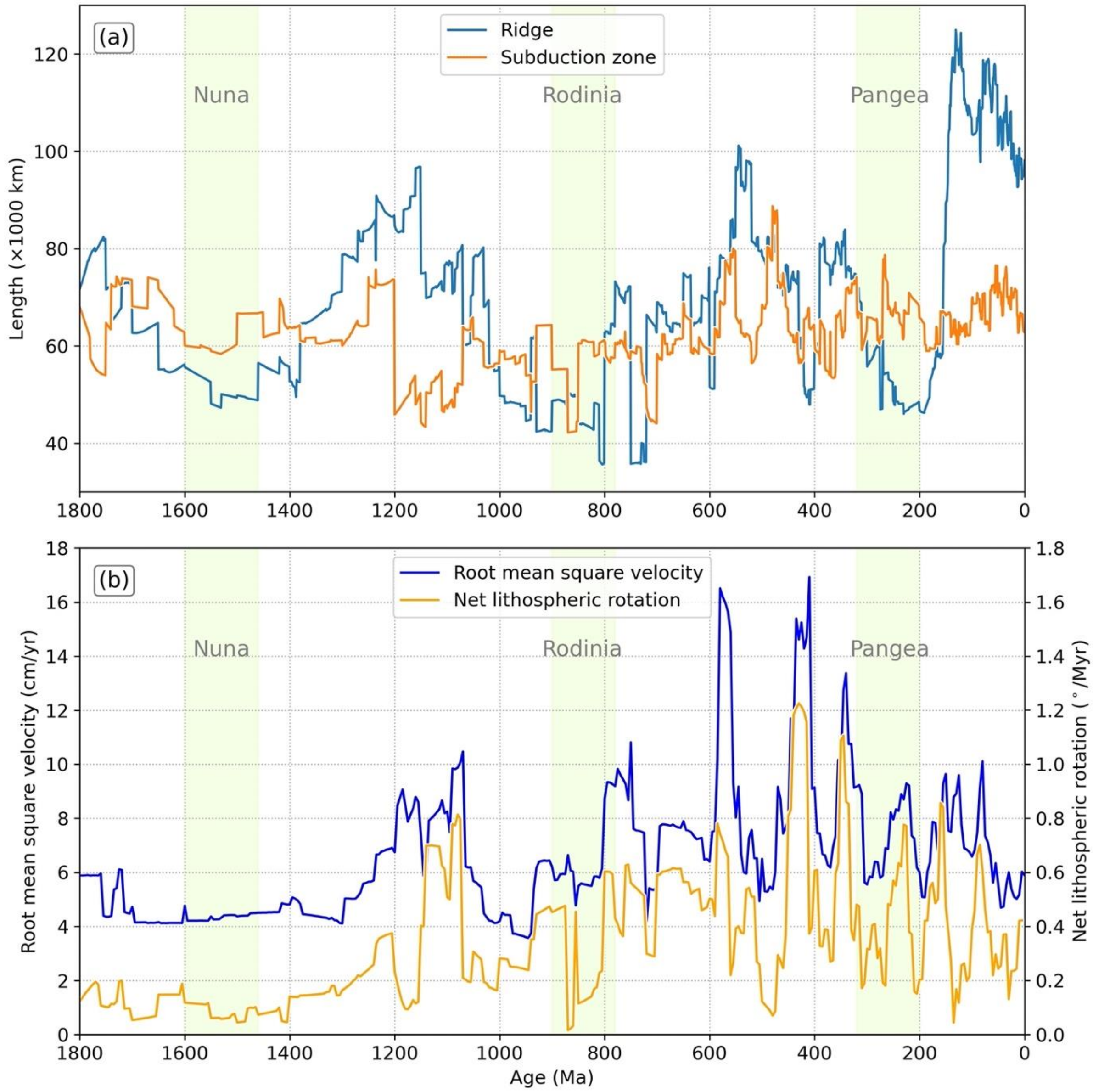

Fig. 15. Geometric and kinematic characteristics of our plate reconstruction. (a) Ridge and subduction zone length through time, the mid-ocean ridge length shows cyclic evolution similar to supercontinents; (b) Net lithospheric rotation and rms speeds of all plates, they display similar trends.

The net lithospheric rotation is generally below 0.2°/Myr between 1.8 and 1.3 Ga, which is smaller than the upper limit of 0.26°/Myr constrained by global azimuthal anisotropy (Conrad and Behn, 2010). However, the net rotation is much larger between 1.3 and 1.0 Ga, peaking at 9°/Myr around 1.1 Ga. These high values partly reflect relatively fast absolute motion of plates while continents are widely dispersed. The root mean square (rms) speeds of all plates before 1.0 Ga are between 4 and 10 cm/yr, which is generally consistent with those of post-Pangean times. The rms speeds tend to be low when supercontinents exist, and high during supercontinent breakup, which reflect the relatively stability of large landmasses (Zahirovic et al., 2015). The rms speeds of all plates through time show similar trends to net lithospheric rotations, indicating that changes in plate speed are partly caused by net rotations. The rms speeds of the plates are expected to be smaller and exhibit less variability over time when net rotations are reduced to below 0.2°/Myr (Müller et al., 2022a).

Attempts to reconstruct Nuna have progressed considerably in the last two decades, from earliest individual snapshots of continental configurations (Zhao et al., 2002), to quantitative kinematic modelling of continents (Pisarevsky et al., 2014), and models with both continental motion and evolving tectonic boundaries (Li et al., 2023, and our new model). Regarding the configuration of Nuna, the positions of some blocks are largely agreed on (Evans, 2013). For instance, the Laurentia-Baltica connection is well constrained by paleomagnetic poles and geological links, Siberia lies offboard present-day northern Laurentia either with a 'gap' (P14 and here with a 'gap' filled by Yangtze) or not (Evans and Mitchell, 2011; Li et al., 2023), Australia-Mawson is located near present-day western Laurentia. However, other blocks are more disputed, such as West Africa-Amazonia, India and South China, and their locations in our reconstruction are different from those of some other models (e.g. Li et al., 2023).

The western margin of Amazonia was an accretionary boundary during the Paleoproterozoic–Mesoproterozoic (Condie et al., 2021) similar to Baltica, which led previous workers to propose a long term 1800−900 Ma Amazonia-Baltica connection (SAMBA reconstruction, Johansson, 2009). However, Fuck et al. (2008) pointed out that the late Paleoproterozoic Ventuari-Tapajós and Rio Negro-Juruena accretionary provinces are truncated by the younger Late Mesoproterozoic orogen in their northern parts, which questions the connectivity of the accretionary belts in Baltica and Amazonia. Moreover, the Putumayo orogeny (Ibañez–Mejia, 2020 and references therein) implies the presence of ocean northwest of Amazonia (in present day coordinates) since at least 1.45 Ga until 1.0–0.95 Ga collision with Baltica. P14 argued that the SAMBA reconstruction is not in good agreement with paleomagnetic data. Li et al. (2023) keep Amazonia and Baltica next to each other in both Nuna and Rodinia, but with different configurations. Here we follow P14 to leave Amazonia out of Nuna, but we recognise that more studies are required to settle this debate.

The hypothesized position of India within Nuna varied considerably in previous studies. It has been tentatively placed near North China (Li et al., 2019; Zhang et al., 2012; Zhao et al., 2002), adjacent to the Sarmatia (southeastern Baltica) in P14, or offboard present-day southern Laurentia (Li et al., 2023). Recent studies have constrained the amalgamation of North and South India to ca. 1.0 Ga (Bhowmik and Santosh, 2019), which means they need to be considered separately for the Paleoproterozoic and Mesoproterozoic. We combine these models, and locate South India next to Sarmatia based on paleomagnetic data and similar accretion history, and North India next to North China.

The locations of Yangtze and Cathaysia (blocks of South China) during the time of Rodinia and Nuna are also controversial (Cawood et al., 2020; Li et al., 2008; Merdith et al., 2017a; Zhao et al., 2002). Some models (‘missing-link’ model) suggest an internal location of South China within Rodinia, placing it between Laurentia and

Australia-Mawson (e.g. Li et al., 2023; Li et al., 2008; Yao et al., 2017). The ca. 1430 Ma granites found on Hainan Island have been correlated with similar granites in western Laurentia, leading to the argument that Cathaysia was located next to present-day western Laurentia within Nuna (e.g. Li et al., 2023; Yao et al., 2017). In Li et al. (2023), Yangtze is located offboard southern Laurentia, and subsequently experienced a dextral motion until accretion with Cathaysia-Laurentia at ca. 900 Ma. To move South China to their outboard positions in Gondwana, these ‘missing-link’ models involve unrealistically-large plate velocities and Euler-pole switches unseen in the Phanerozoic (Merdith et al., 2017b). Other models favour either a peripheral location for South China in Rodinia, or separation from Rodinia (e.g. M21). These models argue that Cathaysia was connected to northern India from at least the Paleoproterozoic, based on similarities in the age distribution of rock units (e.g. Merdith et al., 2017a; Yu et al., 2009). We also note that it is uncertain whether Hainan Island was even part of Cathaysia. Cawood et al. (2020), Pisarevsky et al. (2021) and Zhao et al. (2023) argued that Hainan formed a part of Yangtze before the Paleozoic, and that Yangtze was between northern Laurentia and southern Siberia in Nuna. Here we adopt the latter scenario in alignment with M21.

There are many other debated or unresolved issues for the Proterozoic plate evolution. For instance, the exact configuration of Nuna and Rodinia, and how many cratons were independently drifting outside of them are still disputed. The assembly timing of Nuna was initially proposed at ca. 1.8 Ga based on global-scale orogeny (Zhao et al., 2002), and this timing has been accepted by many studies (e.g. Li et al., 2019; Zhang et al., 2012). In our model, most continents were in close proximity at 1.8 Ga, while the final assembly of Nuna occurred at 1.6 Ga, following recent geochronological studies of Racklan/Isan orogeny (Pourteau et al., 2018; Volante et al., 2020). The breakup timing of Nuna was argued during 1.5–1.25 Ga (Evans and Mitchell, 2011), or soon after ca.1.3 Ga based on paleomagnetic poles (Kirscher et al., 2020; Li et al., 2023). Here we model breakup initially starting at 1460 Ma, with the main breakup phase occurring at ca. 1380 Ma when East Nuna drifted away, which matches well with LIPs records. The discussion above shows many differences between our model and the one presented in Li et al. (2023), for instance the locations of South China, Amazonia-West Africa, and India during the Nuna and Rodinia intervals. We suggest that many of these differences are partly due to our model placing more emphasis on geological data compared to Li et al. (2023). Despite these discrepancies, the two Proterozoic models cover different possibilities, which can be beneficial for conducting uncertainty analysis in future studies (e.g. geodynamic modelling). In addition, the two models are both presented in a paleomagnetic reference frame, implying that the modelled plate motions may incorporate some degree of true polar wander. For example, the gradual counter clockwise rotation of Nuna is attributed to true polar wander by Li et al. (2023). In order to use the plate model in a geodynamic context in future, it is necessary to establish a mantle reference frame that is free of true polar wander.

We present this model as our best attempt at matching the voluminous geological and geophysical data that exists in this context. Contrary to the concept of a "boring billion" (c.f. Holland, 2006), our model reveals a dynamic geological history between 1.8 Ga and 0.8 Ga, which is characterized by supercontinent assembly and breakup, continuous accretion events, and widespread LIP events. We recognise and promote that our model is not perfect and that any part of the model can be queried and improved on using more information, more data, and a better understanding of existing data. As such, this model is a snapshot and a means of presenting and focussing geological questions. We argue that our methodology of focussing on plate interactions and therefore using the wealth of geological information preserved on the continents, is more robust than approaching the problem solely using paleomagnetic data, which are still too scarce to produce unambiguous Precambrian paleogeographic reconstructions in isolation. Ultimately, there is a solution that incorporates all data and we encourage researchers to modify and improve our model. Despite all the caveats required when presenting the results of this ambitious study, we suggest that our model is constrained by considerable data, and that it captures the first-order plate evolution for the last 1.8 billion years. We also keep the plate configurations simple in our model, so that it can be easily refined as additional data become available.

6. Conclusions

We present a new full-plate tectonic reconstruction, with evolving plate boundaries, from 1.8 Ga to present, building on previously published models. We smooth the motion of major plates in the base models to remove unreasonably fast motions, and to improve the match to paleomagnetic poles. The plate boundaries and plate interactions are constrained by magmatic, metamorphic, geochronological and sedimentary data that are interpreted in a tectonic geographic framework to be able to inform the reconstruction. In our model, Nuna formed at 1.6 Ga through the assembly of three landmasses: West Nuna, East Nuna and South Nuna. The North and South Indian blocks are considered separately, with South India juxtaposed southern Baltica, and North India next to North China. Yangtze is located between northern Laurentia and southern Siberia, and Cathaysia is connected to North India. Amazonia, West Africa and West Australia were not part of Nuna. Nuna then broke up mainly between 1.4–1.3 Ga, initially at the north, and propagating towards the south. The breakup timing matches LIPs records. Separated continents came together again to form Rodinia around 930 Ma, which later fragmented at ca. 780 Ma. Our model spans three supercontinents and more than two supercontinent cycles. We have produced a new tectonic framework for analysing the long-term evolution of Earth systems, providing a basis for developing future analysis of tectonic controls on deep Earth resources and developing planetary hypsographic reconstructions that can inform lithosphere/earth surface systems feedbacks.

7. Acknowledgements

XC is funded by National Key R&D Program of China (No. 2022YFF0800401). ASC acknowledges funding through Australian Research Council projects LP210200822, LP200301457, FT120100340 and the MinEx CRC. His contribution forms MinEx publication #xxxx. SL is funded by National Natural Science Foundation of China (No. 42121005, 91958214), Shandong Provincial Natural Science Foundation (No. ZR2021YQ25), and the Marine S&T Fund of Shandong Province for Pilot National Laboratory for Marine Science and Technology (Qingdao) (No. 2022QNLM050302). PSA was supported by the Australian Research Council Laureate Fellowship grant to Z.X. Li (FL150100133). This study is a contribution to IGCP 648. NF acknowledges funding through Australian Research Council project LP170100863.

8. Author contribution statement

XC: Methodology, Investigation, Visualization, Writing – Original Draft. ASC: Investigation, Writing – Review & Editing. PSA: Methodology, Investigation, Writing - Review & Editing. NF: Conceptualization, Investigation, Writing – Review & Editing, Supervision. SL: Investigation, Writing – Review & Editing, Supervision, Funding acquisition. DH: Methodology, Investigation, Writing – Review & Editing. RDM: Conceptualization, Writing – Review & Editing, Resources, Supervision.

9. Data availability

The model will be made publicly available upon publication, and is now available for the reviewers to download at: https://ln5.sync.com/dl/523d23760/3fxtprg5-rgnamhfr-zupkc9ed-ivd564b8.

References

Acharyya, S., 2003. The nature of Mesoproterozoic Central Indian Tectonic Zone with exhumed and reworked older granulites. Gondwana Research, 6(2): 197-214.

Ahmad, M., Scrimgeour, I. and Munson, T., 2013. Geological framework. Geology and Mineral Resources of the Northern Territory. Northern Territory Geological Survey, Special Publication, 5: 1-16.

Antonio, P.Y.J., Baratoux, L., Trindade, R.I.F., Rousse, S., Ayite, A., Lana, C., Macouin, M., Adu, E.W.K., Sanchez, C., Silva, M.A.L., Firmin, A.-S., Martínez Dopico, C.I., Proietti, A., Amponsah, P.O. and Sakyi, P.A., 2021. West Africa in Rodinia: High quality paleomagnetic pole from the ~ 860 Ma Manso dyke swarm (Ghana). Gondwana Research, 94: 28-43.

Austermann, J., Kaye, B.T., Mitrovica, J.X. and Huybers, P., 2014. A statistical analysis of the correlation between large igneous provinces and lower mantle seismic structure. Geophysical Journal International, 197(1): 1-9.

Betts, P.G., Armit, R.J., Stewart, J., Aitken, A.R.A., Ailleres, L., Donchak, P., Hutton, L., Withnall, I. and Giles, D., 2016. Australia and Nuna. Geological Society, London, Special Publications, 424(1): 47-81.

Betts, P.G., Giles, D. and Aitken, A., 2011. Palaeoproterozoic accretion processes of Australia and comparisons with Laurentia. International Geology Review, 53(11-12): 1357-1376.

Bhowmik, S.K. and Santosh, M., 2019. The current status of orogenesis in the Central Indian Tectonic Zone: A view from its Southern Margin. Geological Journal, 54(5): 2912-2934.

Bhowmik, S.K., Wilde, S.A., Bhandari, A., Pal, T. and Pant, N.C., 2012. Growth of the Greater Indian Landmass and its assembly in Rodinia: Geochronological evidence from the Central Indian Tectonic Zone. Gondwana Research, 22(1): 54-72.

Bingen, B., Nordgulen, O. and Viola, G., 2008. A four-phase model for the Sveconorwegian orogeny, SW Scandinavia. Norsk geologisk tidsskrift, 88(1): 43.

Bispo-Santos, F., D'Agrella-Filho, M.S., de Almeida, R.P., Ruiz, A.S., Patroni, O.A. and Silva, J.M., 2023. Paleomagnetic study of the 1112 Ma Huanchaca mafic sills (SW Amazonian Craton, Brazil) and the paleogeographic implications for Rodinia supercontinent. Precambrian Research, 388: 107013.

Bogdanova, S., Pashkevich, I., Gorbatschev, R. and Orlyuk, M., 1996. Riphean rifting and major Palaeoproterozoic crustal boundaries in the basement of the East European Craton: geology and geophysics. Tectonophysics, 268(1-4): 1-21.

Bogdanova, S.V., Bingen, B., Gorbatschev, R., Kheraskova, T.N., Kozlov, V.I., Puchkov, V.N. and Volozh, Y.A., 2008. The East European Craton (Baltica) before and during the assembly of Rodinia. Precambrian Research, 160(1-2): 23-45.

Bradley, D.C., Evans, D.A., O'sullivan, P., Taylor, C.D. and Eglington, B.M., 2022. The Assabet barcode: Mesoproterozoic detrital zircons in Neoproterozoic strata from Mauritania, West Africa. American Journal of Science, 322(8): 939-992.

Brocks, J.J., Jarrett, A.J.M., Sirantoine, E., Hallmann, C., Hoshino, Y. and Liyanage, T., 2017. The rise of algae in Cryogenian oceans and the emergence of animals. Nature, 548(7669): 578-581.

Brown, M. and Johnson, T., 2018. Secular change in metamorphism and the onset of global plate tectonics. American Mineralogist, 103(2): 181-196.

Brown, M., Johnson, T. and Spencer, C.J., 2022. Secular changes in metamorphism and metamorphic cooling rates track the evolving plate-tectonic regime on Earth. Journal of the Geological Society, 179(5): jgs2022-050.

Brown, M., Kirkland, C. and Johnson, T., 2020. Evolution of geodynamics since the Archean: Significant change at the dawn of the Phanerozoic. Geology, 48(5): 488-492.

Burke, K., Steinberger, B., Torsvik, T.H. and Smethurst, M.A., 2008. Plume Generation Zones at the margins of Large Low Shear Velocity Provinces on the core–mantle boundary. Earth and Planetary Science Letters, 265(1-2): 49-60.

Cao, X., Flament, N. and Müller, D., 2021. Coupled Evolution of Plate Tectonics and Basal Mantle Structure. Geochemistry, Geophysics, Geosystems, 22(1): e2020GC009244.

Cawood, P.A. and Korsch, R.J., 2008. Assembling Australia: Proterozoic building of a continent. Precambrian Research, 166(1-4): 1-35.

Cawood, P.A., Strachan, R., Cutts, K., Kinny, P.D., Hand, M. and Pisarevsky, S., 2010. Neoproterozoic orogeny along the margin of Rodinia: Valhalla orogen, North Atlantic. Geology, 38(2): 99-102.

Cawood, P.A., Wang, W., Zhao, T., Xu, Y., Mulder, J.A., Pisarevsky, S.A., Zhang, L., Gan, C., He, H., Liu, H., Qi, L., Wang, Y., Yao, J., Zhao, G., Zhou, M.-F. and Zi, J.-

W., 2020. Deconstructing South China and consequences for reconstructing Nuna and Rodinia. Earth-Science Reviews, 204.

Chappell, B.W. and White, A.J.R., 1974. Two contrasting granite types. Pacif. Geol., 8: 173-174.

Chattopadhyay, A., Bhowmik, S.K. and Roy, A., 2020. Tectonothermal evolution of the Central Indian Tectonic Zone and its implications for Proterozoic supercontinent assembly: the current status. Episodes Journal of International Geoscience, 43(1): 132-144.

Collins, A.S., Blades, M.L., Merdith, A.S. and Foden, J.D., 2021. Closure of the Proterozoic Mozambique Ocean was instigated by a late Tonian plate reorganization event. Communications Earth & Environment, 2(1).

Collins, A.S. and Pisarevsky, S.A., 2005. Amalgamating eastern Gondwana: The evolution of the Circum-Indian Orogens. Earth-Science Reviews, 71(3-4): 229-270.

Condie, K.C., Pisarevsky, S.A. and Puetz, S.J., 2021. LIPs, orogens and supercontinents: The ongoing saga. Gondwana Research, 96: 105-121.

Conrad, C.P. and Behn, M.D., 2010. Constraints on lithosphere net rotation and asthenospheric viscosity from global mantle flow models and seismic anisotropy. Geochemistry, Geophysics, Geosystems, 11(5).

Cook, F.A., Clowes, R.M., Snyder, D.B., van der Velden, A.J., Hall, K.W., Erdmer, P. and Evenchick, C.A., 2004. Precambrian crust beneath the Mesozoic northern Canadian Cordillera discovered by Lithoprobe seismic reflection profiling. Tectonics, 23(2).

Cox, G.M., Collins, A.S., Jarrett, A.J., Blades, M.L., Shannon, A.V., Yang, B., Farkas, J., Hall, P.A., O’Hara, B. and Close, D., 2022. A very unconventional hydrocarbon play: The Mesoproterozoic Velkerri Formation of northern Australia. AAPG Bulletin, 106(6): 1213-1237.

Dasgupta, S., Bose, S. and Das, K., 2013. Tectonic evolution of the Eastern Ghats Belt, India. Precambrian Research, 227: 247-258.

Davies, D.R., Goes, S. and Sambridge, M., 2015. On the relationship between volcanic hotspot locations, the reconstructed eruption sites of large igneous provinces and deep mantle seismic structure. Earth and Planetary Science Letters, 411: 121-130.

de Kock, M.O., Ernst, R., Söderlund, U., Jourdan, F., Hofmann, A., Le Gall, B., Bertrand, H., Chisonga, B.C., Beukes, N., Rajesh, H.M., Moseki, L.M. and Fuchs, R., 2014. Dykes of the 1.11Ga Umkondo LIP, Southern Africa: Clues to a complex plumbing system. Precambrian Research, 249: 129-143.

de Kock, M.O., Evans, D.A.D. and Beukes, N.J., 2009. Validating the existence of Vaalbara in the Neoarchean. Precambrian Research, 174(1-2): 145-154.

Dobmeier, C.J. and Raith, M.M., 2003. Crustal architecture and evolution of the Eastern Ghats Belt and adjacent regions of India. Geological Society, London, Special Publications, 206(1): 145-168.

Domeier, M. and Torsvik, T.H., 2017. Full-plate modelling in pre-Jurassic time. Geological Magazine, 156(2): 261-280.

Doughty, P.T. and Chamberlain, K.R., 1996. Salmon River Arch revisited: new evidence for 1370 Ma rifting near the end of deposition in the Middle Proterozoic Belt basin. Canadian Journal of Earth Sciences, 33(7): 1037-1052.

Eglington, B.M., Pehrsson, S.J., Ansdell, K.M., Lescuyer, J.L., Quirt, D., Milesi, J.P. and Brown, P., 2013. A domain-based digital summary of the evolution of the

Palaeoproterozoic of North America and Greenland and associated unconformity-related uranium mineralization. Precambrian Research, 232: 4-26.

Elming, S.-Å. and Mattsson, H., 2001. Post Jotnian basic intrusions in the Fennoscandian Shield, and the break up of Baltica from Laurentia: a palaeomagnetic and AMS study. Precambrian Research, 108(3-4): 215-236.

Ernst, R.E., Hamilton, M.A., Söderlund, U., Hanes, J.A., Gladkochub, D.P., Okrugin, A.V., Kolotilina, T., Mekhonoshin, A.S., Bleeker, W., LeCheminant, A.N., Buchan, K.L., Chamberlain, K.R. and Didenko, A.N., 2016. Long-lived connection between southern Siberia and northern Laurentia in the Proterozoic. Nature Geoscience, 9(6): 464-469.

Ernst, R.E., Pereira, E., Hamilton, M.A., Pisarevsky, S.A., Rodriques, J., Tassinari, C.C.G., Teixeira, W. and Van-Dunem, V., 2013. Mesoproterozoic intraplate magmatic ‘barcode’ record of the Angola portion of the Congo Craton: Newly dated magmatic events at 1505 and 1110Ma and implications for Nuna (Columbia) supercontinent reconstructions. Precambrian Research, 230: 103-118.

Evans, D.A., 2009. The palaeomagnetically viable, long-lived and all-inclusive Rodinia supercontinent reconstruction. Geological Society, London, Special Publications, 327(1): 371-404.

Evans, D.A., 2013. Reconstructing pre-Pangean supercontinents. Bulletin, 125(11-12): 1735-1751.

Evans, D.A.D. and Mitchell, R.N., 2011. Assembly and breakup of the core of Paleoproterozoic-Mesoproterozoic supercontinent Nuna. Geology, 39(5): 443-446.

Flament, N., Bodur, O.F., Williams, S.E. and Merdith, A.S., 2022. Assembly of the basal mantle structure beneath Africa. Nature, 603(7903): 846-851.

Frost, B.R., Barnes, C.G., Collins, W.J., Arculus, R.J., Ellis, D.J. and Frost, C.D., 2001. A geochemical classification for granitic rocks. Journal of petrology, 42(11): 2033-2048.

Frost, D.A. and Rost, S., 2014. The P-wave boundary of the Large-Low Shear Velocity Province beneath the Pacific. Earth and Planetary Science Letters, 403: 380-392.

Fuck, R.A., Brito Neves, B.B. and Schobbenhaus, C., 2008. Rodinia descendants in South America. Precambrian Research, 160(1-2): 108-126.

Furlanetto, F., Thorkelson, D., Rainbird, R., Davis, W., Gibson, H. and Marshall, D., 2016. The Paleoproterozoic Wernecke Supergroup of Yukon, Canada: Relationships to orogeny in northwestern Laurentia and basins in North America, East Australia, and China. Gondwana Research, 39: 14-40.

Furlanetto, F., Thorkelson, D.J., Gibson, H.D., Marshall, D.D., Rainbird, R.H., Davis, W.J., Crowley, J.L. and Vervoort, J.D., 2013. Late Paleoproterozoic terrane accretion in northwestern Canada and the case for circum-Columbian orogenesis. Precambrian Research, 224: 512-528.

Gardiner, N.J., Maidment, D.W., Kirkland, C.L., Bodorkos, S., Smithies, R.H. and Jeon, H., 2018. Isotopic insight into the Proterozoic crustal evolution of the Rudall Province, Western Australia. Precambrian Research, 313: 31-50.

Garnero, E.J. and McNamara, A.K., 2008. Structure and dynamics of Earth's lower mantle. science, 320(5876): 626-628.

Ge, R., Zhu, W., Wilde, S.A., He, J. and Cui, X., 2015. Synchronous crustal growth and reworking recorded in late Paleoproterozoic granitoids in the northern Tarim craton: In situ zircon U-Pb-Hf-O isotopic and geochemical constraints and tectonic implications. Geological Society of America Bulletin, 127(5-6): 781-803.

Gernon, T.M., Hincks, T.K., Merdith, A.S., Rohling, E.J., Palmer, M.R., Foster, G.L., Bataille, C.P. and Müller, R.D., 2021. Global chemical weathering dominated by continental arcs since the mid-Palaeozoic. Nature Geoscience, 14(9): 690-696.

Goddéris, Y., Donnadieu, Y., Carretier, S., Aretz, M., Dera, G., Macouin, M. and Regard, V., 2017. Onset and ending of the late Palaeozoic ice age triggered by tectonically paced rock weathering. Nature Geoscience, 10(5): 382-386.

Goddéris, Y., Donnadieu, Y. and Mills, B.J.W., 2023. What Models Tell Us About the Evolution of Carbon Sources and Sinks over the Phanerozoic. Annual Review of Earth and Planetary Sciences, 51(1): 471-492.

Goodge, J.W., Fanning, C.M., Fisher, C.M. and Vervoort, J.D., 2017. Proterozoic crustal evolution of central East Antarctica: Age and isotopic evidence from glacial igneous clasts, and links with Australia and Laurentia. Precambrian Research, 299: 151-176.

Gurnis, M., 1988. Large-scale mantle convection and the aggregation and dispersal of supercontinents. Nature, 332(6166): 695-699.

Haines, P.W., Kirkland, C.L., Wingate, M.T.D., Allen, H., Belousova, E.A. and Gréau, Y., 2016. Tracking sediment dispersal during orogenesis: A zircon age and Hf isotope study from the western Amadeus Basin, Australia. Gondwana Research, 37: 324-347.

Harley, S., 2003. Archaean-Cambrian crustal development of East Antarctica: metamorphic characteristics and tectonic implications. Geological Society, London, Special Publications, 206(1): 203-230.

Harms, T.A., Brady, J.B., Burger, H.R. and Cheney, J.T., 2004. Advances in the geology of the Tobacco Root Mountains, Montana, and their implications for the history of the northern Wyoming province. Geological Society of America.

Hasterok, D., Halpin, J.A., Collins, A.S., Hand, M., Kreemer, C., Gard, M.G. and Glorie, S., 2022. New Maps of Global Geological Provinces and Tectonic Plates. Earth-Science Reviews, 231.

He, Y., Zhao, G., Sun, M. and Xia, X., 2009. SHRIMP and LA-ICP-MS zircon geochronology of the Xiong'er volcanic rocks: Implications for the Paleo-Mesoproterozoic evolution of the southern margin of the North China Craton. Precambrian Research, 168(3-4): 213-222.

Henderson, B., Collins, A.S., Payne, J., Forbes, C. and Saha, D., 2014. Geologically constraining India in Columbia: The age, isotopic provenance and geochemistry of the protoliths of the Ongole Domain, Southern Eastern Ghats, India. Gondwana Research, 26(3-4): 888-906.

Hoffman, P.F., 1991. Did the breakout of Laurentia turn Gondwanaland inside-out? Science, 252(5011): 1409-1412.

Hoffman, P.F., 1997. Tectonic genealogy of North America. Earth structure: An introduction to structural geology and tectonics.: 459-464.

Holland, H.D., 2006. The oxygenation of the atmosphere and oceans. Philosophical Transactions of the Royal Society B: Biological Sciences, 361(1470): 903-915.

Howard, H.M., Smithies, R.H., Kirkland, C.L., Kelsey, D.E., Aitken, A., Wingate, M.T.D., Quentin de Gromard, R., Spaggiari, C.V. and Maier, W.D., 2015. The burning heart — The Proterozoic geology and geological evolution of the west Musgrave Region, central Australia. Gondwana Research, 27(1): 64-94.

Ibañez–Mejia, M., 2020. The Putumayo orogen of Amazonia: a synthesis. Gómez. J. and Mateus.

Jacobs, J., Pisarevsky, S., Thomas, R.J. and Becker, T., 2008. The Kalahari Craton during the assembly and dispersal of Rodinia. Precambrian Research, 160(1-2): 142-158.

Johansson, Å., 2009. Baltica, Amazonia and the SAMBA connection—1000 million years of neighbourhood during the Proterozoic? Precambrian Research, 175(1-4): 221-234.

Johnson, S.P., Sheppard, S., Rasmussen, B., Wingate, M.T.D., Kirkland, C.L., Muhling, J.R., Fletcher, I.R. and Belousova, E.A., 2011. Two collisions, two sutures: Punctuated pre-1950Ma assembly of the West Australian Craton during the Ophthalmian and Glenburgh Orogenies. Precambrian Research, 189(3-4): 239-262.

Karlsen, K.S., Conrad, C.P. and Magni, V., 2019. Deep Water Cycling and Sea Level Change Since the Breakup of Pangea. Geochemistry, Geophysics, Geosystems, 20(6): 2919-2935.

Karlstrom, K.E., Åhäll, K.-I., Harlan, S.S., Williams, M.L., McLelland, J. and Geissman, J.W., 2001. Long-lived (1.8–1.0 Ga) convergent orogen in southern Laurentia, its extensions to Australia and Baltica, and implications for refining Rodinia. Precambrian research, 111(1-4): 5-30.

Kirscher, U., Mitchell, R.N., Liu, Y., Nordsvan, A.R., Cox, G.M., Pisarevsky, S.A., Wang, C., Wu, L., Murphy, J.B. and Li, Z.-X., 2020. Paleomagnetic constraints on the duration of the Australia-Laurentia connection in the core of the Nuna supercontinent. Geology, 49(2): 174-179.

Kirscher, U., Mitchell, R.N., Liu, Y., Nordsvan, A.R., Cox, G.M., Pisarevsky, S.A., Wang, C., Wu, L., Murphy, J.B. and Li, Z.-X., 2021. Paleomagnetic constraints on the duration of the Australia-Laurentia connection in the core of the Nuna supercontinent. Geology, 49(2): 174-179.

Kirscher, U., Mitchell, R.N., Liu, Y., Pisarevsky, S.A., Giddings, J. and Li, Z.X., 2022. Paleomagnetic Evidence for a Paleoproterozoic Rotational Assembly of the North Australian Craton in the Leadup to Supercontinent Formation. Geophysical Research Letters, 49(22).

Korsch, R.J., Huston, D.L., Henderson, R.A., Blewett, R.S., Withnall, I.W., Fergusson, C.L., Collins, W.J., Saygin, E., Kositcin, N., Meixner, A.J., Chopping, R., Henson, P.A., Champion, D.C., Hutton, L.J., Wormald, R., Holzschuh, J. and Costelloe, R.D., 2012. Crustal architecture and geodynamics of North Queensland, Australia: Insights from deep seismic reflection profiling. Tectonophysics, 572-573: 76-99.

Li, S., Li, X., Wang, G., Liu, Y., Wang, Z., Wang, T., Cao, X., Guo, X., Somerville, I., Li, Y., Zhou, J., Dai, L., Jiang, S., Zhao, H., Wang, Y., Wang, G. and Yu, S., 2019. Global Meso-Neoproterozoic plate reconstruction and formation mechanism for Precambrian basins: Constraints from three cratons in China. Earth-Science Reviews, 198: 102946.

Li, S., Suo, Y., Li, X., Liu, B., Dai, L., Wang, G., Zhou, J., Li, Y., Liu, Y., Cao, X., Somerville, I., Mu, D., Zhao, S., Liu, J., Meng, F., Zhen, L., Zhao, L., Zhu, J., Yu, S., Liu, Y. and Zhang, G., 2018. Microplate tectonics: new insights from micro-blocks in the global oceans, continental margins and deep mantle. Earth-Science Reviews, 185: 1029-1064.

Li, Z.-X., Liu, Y. and Ernst, R., 2023. A dynamic 2000—540 Ma Earth history: From cratonic amalgamation to the age of supercontinent cycle. Earth-Science Reviews, 238.

Li, Z.X., Bogdanova, S.V., Collins, A.S., Davidson, A., De Waele, B., Ernst, R.E., Fitzsimons, I.C.W., Fuck, R.A., Gladkochub, D.P., Jacobs, J., Karlstrom, K.E., Lu, S., Natapov, L.M., Pease, V., Pisarevsky, S.A., Thrane, K. and Vernikovsky, V., 2008.

Assembly, configuration, and break-up history of Rodinia: A synthesis. Precambrian Research, 160(1-2): 179-210.

Litherland, M. and Power, G., 1989. The geologic and geomorphologic evolution of Serrania Huanchaca, eastern Bolivia: The legendary “Lost World”. Journal of South American Earth Sciences, 2(1): 1-17.

Liu, Q., Yu, J.-H., O’Reilly, S., Zhou, M.-F., Griffin, W., Wang, L. and Cui, X., 2014. Origin and geological significance of Paleoproterozoic granites in the northeastern Cathaysia Block, South China. Precambrian Research, 248: 72-95.

Long, S., McQuarrie, N., Tobgay, T., Rose, C., Gehrels, G. and Grujic, D., 2011. Tectonostratigraphy of the Lesser Himalaya of Bhutan: Implications for the along-strike stratigraphic continuity of the northern Indian margin. Bulletin, 123(7-8): 1406-1426.

McQuarrie, N., Robinson, D., Long, S., Tobgay, T., Grujic, D., Gehrels, G. and Ducea, M., 2008. Preliminary stratigraphic and structural architecture of Bhutan: Implications for the along strike architecture of the Himalayan system. Earth and Planetary Science Letters, 272(1-2): 105-117.

Medig, K., Thorkelson, D. and Dunlop, R., 2009. The Proterozoic Pinguicula Group: stratigraphy, contact relationships and possible correlations. Yukon exploration and geology: 265-278.

Meert, J.G., Hargraves, R.B., Van der Voo, R., Hall, C.M. and Halliday, A.N., 1994. Paleomagnetic and 40Ar/39Ar studies of late Kibaran intrusives in Burundi, East Africa: implications for late Proterozoic supercontinents. The Journal of Geology, 102(6): 621-637.

Meert, J.G. and Santosh, M., 2022. The Columbia supercontinent: Retrospective, status, and a statistical assessment of paleomagnetic poles used in reconstructions. Gondwana Research, 110: 143-164.

Merdith, A.S., Collins, A.S., Williams, S.E., Pisarevsky, S., Foden, J.D., Archibald, D.B., Blades, M.L., Alessio, B.L., Armistead, S., Plavsa, D., Clark, C. and Müller, R.D., 2017a. A full-plate global reconstruction of the Neoproterozoic. Gondwana Research, 50: 84-134.

Merdith, A.S., Williams, S.E., Collins, A.S., Tetley, M.G., Mulder, J.A., Blades, M.L., Young, A., Armistead, S.E., Cannon, J., Zahirovic, S. and Müller, R.D., 2021. Extending full-plate tectonic models into deep time: Linking the Neoproterozoic and the Phanerozoic. Earth-Science Reviews, 214: 103477.

Merdith, A.S., Williams, S.E., Müller, R.D. and Collins, A.S., 2017b. Kinematic constraints on the Rodinia to Gondwana transition. Precambrian Research, 299: 132-150.

Miller, C., Klötzli, U., Frank, W., Thöni, M. and Grasemann, B., 2000. Proterozoic crustal evolution in the NW Himalaya (India) as recorded by circa 1.80 Ga mafic and 1.84 Ga granitic magmatism. Precambrian Research, 103(3-4): 191-206.

Mills, B.J.W., Krause, A.J., Jarvis, I. and Cramer, B.D., 2023. Evolution of Atmospheric O2 Through the Phanerozoic, Revisited. Annual Review of Earth and Planetary Sciences, 51(1): 253-276.

Mitchell, R.N., Kilian, T.M. and Evans, D.A., 2012. Supercontinent cycles and the calculation of absolute palaeolongitude in deep time. Nature, 482(7384): 208-11.

Mitchelmore, M.D. and Cook, F.A., 1994. Inversion of the Proterozoic Wernecke basin during tectonic development of the Racklan Orogen, northwest Canada. Canadian Journal of Earth Sciences, 31(3): 447-457.

Morrissey, L.J., Barovich, K.M., Hand, M., Howard, K.E. and Payne, J.L., 2019. Magmatism and metamorphism at ca. 1.45 Ga in the northern Gawler Craton: The Australian record of rifting within Nuna (Columbia). Geoscience Frontiers, 10(1): 175-194.

Morrissey, L.J., Payne, J.L., Hand, M., Clark, C. and Janicki, M., 2023. One billion years of tectonism at the Paleoproterozoic interface of North and South Australia. Precambrian Research, 393.

Morrissey, L.J., Payne, J.L., Hand, M., Clark, C., Taylor, R., Kirkland, C.L. and Kylander-Clark, A., 2017. Linking the Windmill Islands, east Antarctica and the Albany–Fraser Orogen: Insights from U–Pb zircon geochronology and Hf isotopes. Precambrian Research, 293: 131-149.

Mukherjee, I. and Large, R.R., 2020. Co-evolution of trace elements and life in Precambrian oceans: The pyrite edition. Geology, 48(10): 1018-1022.

Mulder, J.A., Karlstrom, K.E., Halpin, J.A., Merdith, A.S., Spencer, C.J., Berry, R.F. and McDonald, B., 2018. Rodinian devil in disguise: Correlation of 1.25–1.10 Ga strata between Tasmania and Grand Canyon. Geology, 46(11): 991-994.

Müller, R.D., Cannon, J., Qin, X., Watson, R.J., Gurnis, M., Williams, S., Pfaffelmoser, T., Seton, M., Russell, S.H.J. and Zahirovic, S., 2018. GPlates: Building a Virtual Earth Through Deep Time. Geochemistry, Geophysics, Geosystems, 19(7): 2243-2261.

Müller, R.D., Flament, N., Cannon, J., Tetley, M.G., Williams, S.E., Cao, X., Bodur, Ö.F., Zahirovic, S. and Merdith, A., 2022a. A tectonic-rules-based mantle reference frame since 1 billion years ago – implications for supercontinent cycles and plate–mantle system evolution. Solid Earth, 13(7): 1127-1159.

Müller, R.D., Mather, B., Dutkiewicz, A., Keller, T., Merdith, A., Gonzalez, C.M., Gorczyk, W. and Zahirovic, S., 2022b. Evolution of Earth's tectonic carbon conveyor belt. Nature, 605(7911): 629-639.

Müller, R.D., Seton, M., Zahirovic, S., Williams, S.E., Matthews, K.J., Wright, N.M., Shephard, G.E., Maloney, K.T., Barnett-Moore, N., Hosseinpour, M., Bower, D.J. and Cannon, J., 2016. Ocean Basin Evolution and Global-Scale Plate Reorganization Events Since Pangea Breakup. Annual Review of Earth and Planetary Sciences, 44(1): 107-138.

Murphy, J.B. and Nance, R.D., 2003. Do supercontinents introvert or extrovert?: Sm-Nd isotope evidence. Geology, 31(10): 873-876.

Nance, R.D., Murphy, J.B. and Santosh, M., 2014. The supercontinent cycle: A retrospective essay. Gondwana Research, 25(1): 4-29.

Nixon, A.L., Glorie, S., Collins, A.S., Blades, M.L., Simpson, A. and Whelan, J.A., 2022. Inter-cratonic geochronological and geochemical correlations of the Derim Derim–Galiwinku/Yanliao reconstructed Large Igneous Province across the North Australian and North China cratons. Gondwana Research, 103: 473-486.

Nordsvan, A.R., Collins, W.J., Li, Z.-X., Spencer, C.J., Pourteau, A., Withnall, I.W., Betts, P.G. and Volante, S., 2018. Laurentian crust in northeast Australia: Implications for the assembly of the supercontinent Nuna. Geology, 46(3): 251-254.

Occhipinti, S.A., Sheppard, S., Passchier, C., Tyler, I.M. and Nelson, D.R., 2004. Palaeoproterozoic crustal accretion and collision in the southern Capricorn Orogen: the Glenburgh Orogeny. Precambrian Research, 128(3-4): 237-255.

Park, R., 1992. Plate kinematic history of Baltica during the Middle to Late Proterozoic: a model. Geology, 20(8): 725-728.

Pesonen, L., Elming, S.-Å., Mertanen, S., Pisarevsky, S., D'Agrella-Filho, M., Meert, J., Schmidt, P., Abrahamsen, N. and Bylund, G., 2003. Palaeomagnetic configuration of continents during the Proterozoic. Tectonophysics, 375(1-4): 289-324.

Pisarevsky, S. and Bylund, G., 2010. Paleomagnetism of 1780–1770 Ma mafic and composite intrusions of Småland (Sweden): implications for the Mesoproterozoic supercontinent. American Journal of Science, 310(9): 1168-1186.

Pisarevsky, S. and Natapov, L., 2003. Siberia and rodinia. Tectonophysics, 375(1-4): 221-245.

Pisarevsky, S., Natapov, L., Donskaya, T., Gladkochub, D. and Vernikovsky, V., 2008. Proterozoic Siberia: a promontory of Rodinia. Precambrian research, 160(1-2): 66-76.

Pisarevsky, S.A., Biswal, T.K., Wang, X.-C., De Waele, B., Ernst, R., Söderlund, U., Tait, J.A., Ratre, K., Singh, Y.K. and Cleve, M., 2013. Palaeomagnetic, geochronological and geochemical study of Mesoproterozoic Lakhna Dykes in the Bastar Craton, India: Implications for the Mesoproterozoic supercontinent. Lithos, 174: 125-143.

Pisarevsky, S.A., Elming, S.-Å., Pesonen, L.J. and Li, Z.-X., 2014. Mesoproterozoic paleogeography: Supercontinent and beyond. Precambrian Research, 244: 207-225.

Pisarevsky, S.A., Gladkochub, D.P. and Donskaya, T.V., 2021. Precambrian paleogeography of Siberia, Ancient Supercontinents and the Paleogeography of Earth. Elsevier, pp. 263-275.

Pisarevsky, S.A., Li, Z.X., Tetley, M.G., Liu, Y. and Beardmore, J.P., 2022. An updated internet-based Global Paleomagnetic Database. Earth-Science Reviews, 235.

Pisarevsky, S.A., Wingate, M.T., Powell, C.M., Johnson, S. and Evans, D.A., 2003. Models of Rodinia assembly and fragmentation. Geological Society, London, Special Publications, 206(1): 35-55.

Pourteau, A., Smit, M.A., Li, Z., Collins, W.J., Nordsvan, A.R., Volante, S. and Li, J., 2018. 1.6 Ga crustal thickening along the final Nuna suture. Geology, 46(11): 959-962.

Rawlings, D., 1999. Stratigraphic resolution of a multiphase intracratonic basin system: the McArthur Basin, northern Australia. Australian Journal of Earth Sciences, 46(5): 703-723.

Richards, A., Argles, T., Harris, N., Parrish, R., Ahmad, T., Darbyshire, F. and Draganits, E., 2005. Himalayan architecture constrained by isotopic tracers from clastic sediments. Earth and Planetary Science Letters, 236(3-4): 773-796.

Rickers, K., Mezger, K. and Raith, M.M., 2001. Evolution of the continental crust in the Proterozoic Eastern Ghats Belt, India and new constraints for Rodinia reconstruction: implications from Sm–Nd, Rb–Sr and Pb–Pb isotopes. Precambrian Research, 112(3-4): 183-210.

Roberts, N.M., Salminen, J., Johansson, Å., Mitchell, R.N., Palin, R.M., Condie, K.C. and Spencer, C.J., 2022. On the enigmatic mid-Proterozoic: Single-lid versus plate tectonics. Earth and Planetary Science Letters, 594: 117749.

Rogers, J.J.W. and Santosh, M., 2002. Configuration of Columbia, a Mesoproterozoic Supercontinent. Gondwana Research, 5(1): 5-22.

Ross, G., Villeneuve, M. and Theriault, R., 2001. Isotopic provenance of the lower Muskwa assemblage (Mesoproterozoic, Rocky Mountains, British Columbia): New clues to correlation and source areas. Precambrian Research, 111(1-4): 57-77.

Ross, G.M., Parrish, R.R. and Winston, D., 1992. Provenance and U-Pb geochronology of the Mesoproterozoic Belt Supergroup (northwestern United States): Implications for age of deposition and pre-Panthalassa plate reconstructions. Earth and Planetary Science Letters, 113(1-2): 57-76.

Salminen, J., Hanson, R., Evans, D.A.D., Gong, Z., Larson, T., Walker, O., Gumsley, A., Söderlund, U. and Ernst, R., 2018. Direct Mesoproterozoic connection of the Congo and Kalahari cratons in proto-Africa: Strange attractors across supercontinental cycles. Geology, 46(11): 1011-1014.

Salminen, J. and Pesonen, L.J., 2007. Paleomagnetic and rock magnetic study of the Mesoproterozoic sill, Valaam island, Russian Karelia. Precambrian Research, 159(3-4): 212-230.

Salminen, J., Pesonen, L.J., Mertanen, S., Vuollo, J. and Airo, M.-L., 2009. Palaeomagnetism of the Salla Diabase Dyke, northeastern Finland, and its implication for the Baltica-Laurentia entity during the Mesoproterozoic. Geological Society, London, Special Publications, 323(1): 199-217.

Santos, J.O.S., Hartmann, L.A., Gaudette, H.E., Groves, D.I., Mcnaughton, N.J. and Fletcher, I.R., 2000. A new understanding of the provinces of the Amazon Craton based on integration of field mapping and U-Pb and Sm-Nd geochronology. Gondwana Research, 3(4): 453-488.

Seton, M., Müller, R.D., Zahirovic, S., Gaina, C., Torsvik, T., Shephard, G., Talsma, A., Gurnis, M., Turner, M., Maus, S. and Chandler, M., 2012. Global continental and ocean basin reconstructions since 200Ma. Earth-Science Reviews, 113(3-4): 212-270.

Seton, M., Williams, S.E., Domeier, M., Collins, A.S. and Sigloch, K., 2023. Deconstructing plate tectonic reconstructions. Nature Reviews Earth & Environment, 4(3): 185-204.

Spaggiari, C.V., Smithies, R.H., Kirkland, C.L., Wingate, M.T.D., England, R.N. and Lu, Y.-J., 2018. Buried but preserved: The Proterozoic Arubiddy Ophiolite, Madura Province, Western Australia. Precambrian Research, 317: 137-158.

Spencer, C.J., 2022. Biogeodynamics: Coupled evolution of the biosphere, atmosphere, and lithosphere. Geology, 50(8): 867-868.

Starmer, I.C., 1996. Accretion, rifting, rotation and collision in the North Atlantic supercontinent, 1700-950 Ma. Geological Society, London, Special Publications, 112(1): 219-248.

Stern, R.J., 2018. The evolution of plate tectonics. Philosophical Transactions of the Royal Society A: Mathematical, Physical and Engineering Sciences, 376(2132): 20170406.

Swanson-Hysell, N.L., Kilian, T.M. and Hanson, R.E., 2015. A new grand mean palaeomagnetic pole for the 1.11 Ga Umkondo large igneous province with implications for palaeogeography and the geomagnetic field. Geophysical Journal International, 203(3): 2237-2247.

Tamblyn, R., Hasterok, D., Hand, M. and Gard, M., 2021. Mantle heating at ca. 2 Ga by continental insulation: Evidence from granites and eclogites. Geology, 50(1): 91-95.

Tamblyn, R., Hasterok, D., Hand, M. and Gard, M., 2022. Mantle heating at ca. 2 Ga by continental insulation: Evidence from granites and eclogites. Geology, 50(1): 91-95.

Thorkelson, D.J., Abbott, J.G., Mortensen, J.K., Creaser, R.A., Villeneuve, M.E., McNicoll, V.J. and Layer, P.W., 2005. Early and middle Proterozoic evolution of Yukon, Canada. Canadian Journal of Earth Sciences, 42(6): 1045-1071.

Thorkelson, D.J., Mortensen, J.K., Creaser, R.A., Davidson, G.J. and Abbott, J.G., 2001. Early Proterozoic magmatism in Yukon, Canada: constraints on the evolution of northwestern Laurentia. Canadian Journal of Earth Sciences, 38(10): 1479-1494.

Tohver, E., Pluijm, B.A.v.d., Mezger, K., Scandolara, J.E. and Essene, E.J., 2005a. Two stage tectonic history of the SW Amazon craton in the late Mesoproterozoic: identifying a cryptic suture zone. Precambrian Research, 137(1-2): 35-59.

Tohver, E., Van Der Pluijm, B., Scandolara, J. and Essene, E., 2005b. Late Mesoproterozoic deformation of SW Amazonia (Rondônia, Brazil): geochronological and structural evidence for collision with southern Laurentia. The Journal of Geology, 113(3): 309-323.

Tohver, E., Van der Pluijm, B., Van der Voo, R., Rizzotto, G. and Scandolara, J., 2002. Paleogeography of the Amazon craton at 1.2 Ga: early Grenvillian collision with the Llano segment of Laurentia. Earth and Planetary Science Letters, 199(1-2): 185-200.

Torsvik, T.H., Burke, K., Steinberger, B., Webb, S.J. and Ashwal, L.D., 2010. Diamonds sampled by plumes from the core-mantle boundary. Nature, 466(7304): 352-5.

Torsvik, T.H. and Cocks, L.R.M., 2017. The integration of palaeomagnetism, the geological record and mantle tomography in the location of ancient continents. Geological Magazine, 156(2): 242-260.

Upton, B., Rämö, O.T., Heaman, L., Blichert-Toft, J., Kalsbeek, F., Barry, T. and Jepsen, H., 2005. The Mesoproterozoic Zig-Zag Dal basalts and associated intrusions of eastern North Greenland: mantle plume–lithosphere interaction. Contributions to Mineralogy and Petrology, 149: 40-56.

Volante, S., Pourteau, A., Collins, W.J., Blereau, E., Li, Z.X., Smit, M., Evans, N.J., Nordsvan, A.R., Spencer, C.J., McDonald, B.J., Li, J. and Günter, C., 2020. Multiple P–T–d–t paths reveal the evolution of the final Nuna assembly in northeast Australia. Journal of Metamorphic Geology, 38(6): 593-627.

Wang, C., Li, Z.X., Peng, P., Pisarevsky, S., Liu, Y., Kirscher, U. and Nordsvan, A., 2019. Long-lived connection between the North China and North Australian cratons in supercontinent Nuna: paleomagnetic and geological constraints. Sci Bull (Beijing), 64(13): 873-876.

Wang, L.-J., Yu, J.-H., Griffin, W. and O'Reilly, S., 2012. Early crustal evolution in the western Yangtze Block: evidence from U–Pb and Lu–Hf isotopes on detrital zircons from sedimentary rocks. Precambrian Research, 222: 368-385.

Wang, P., Zhao, G., Liu, Q., Han, Y., Yao, J. and Li, J., 2020. Zircons from the Tarim basement provide insights into its positions in Columbia and Rodinia supercontinents. Precambrian Research, 341.

Wang, W., Cawood, P.A. and Pandit, M.K., 2021. India in the Nuna to Gondwana supercontinent cycles: Clues from the north Indian and Marwar Blocks. American Journal of Science, 321(1-2): 83-117.

Wang, W., Cawood, P.A., Zhou, M.-F. and Zhao, J.-H., 2016. Paleoproterozoic magmatic and metamorphic events link Yangtze to northwest Laurentia in the Nuna supercontinent. Earth and Planetary Science Letters, 433: 269-279.

Wang, W. and Zhou, M.-F., 2014. Provenance and tectonic setting of the Paleo- to Mesoproterozoic Dongchuan Group in the southwestern Yangtze Block, South China: implication for the breakup of the supercontinent Columbia. Tectonophysics, 610: 110-127.

Whitmeyer, S.J. and Karlstrom, K.E., 2007. Tectonic model for the Proterozoic growth of North America. Geosphere, 3(4): 220-259.

Williams, H., Hoffman, P.F., Lewry, J.F., Monger, J.W. and Rivers, T., 1991. Anatomy of North America: thematic geologic portrayals of the continent. Tectonophysics, 187(1-3): 117-134.

Wrobel-Daveau, J.-C., Nicoll, G., Tetley, M.G., Gréselle, B., Perez-Diaz, L., Davies, A. and Eglington, B.M., 2022. Plate tectonic modelling and the energy transition. Earth-Science Reviews, 234.

Xu, Y.-J., Cawood, P.A. and Du, Y.-S., 2016. Intraplate orogenesis in response to Gondwana assembly: Kwangsian orogeny, South China. American Journal of Science, 316(4): 329-362.

Yang, B., Collins, A.S., Blades, M.L. and Jourdan, F., 2023. Orogens and detritus: unravelling the Mesoproterozoic tectonic geography of northern Australia through coupled detrital thermo- and geo-chronometers. Australian Journal of Earth Sciences: 1-19.

Yang, B., Collins, A.S., Blades, M.L., Munson, T.J., Payne, J.L., Glorie, S. and Farkaš, J., 2020. Tectonic controls on sedimentary provenance and basin geography of the Mesoproterozoic Wilton package, McArthur Basin, northern Australia. Geological Magazine, 159(2): 179-198.

Yao, W., Li, Z.-X., Li, W.-X. and Li, X.-H., 2017. Proterozoic tectonics of Hainan Island in supercontinent cycles: New insights from geochronological and isotopic results. Precambrian Research, 290: 86-100.

Young, A., Flament, N., Maloney, K., Williams, S., Matthews, K., Zahirovic, S. and Müller, R.D., 2019. Global kinematics of tectonic plates and subduction zones since the late Paleozoic Era. Geoscience Frontiers, 10(3): 989-1013.

Yu, J.-H., O'Reilly, S.Y., Zhou, M.-F., Griffin, W. and Wang, L., 2012. U–Pb geochronology and Hf–Nd isotopic geochemistry of the Badu Complex, Southeastern China: implications for the Precambrian crustal evolution and paleogeography of the Cathaysia Block. Precambrian Research, 222: 424-449.

Yu, J.-H., Wang, L., O'reilly, S., Griffin, W., Zhang, M., Li, C. and Shu, L., 2009. A Paleoproterozoic orogeny recorded in a long-lived cratonic remnant (Wuyishan terrane), eastern Cathaysia Block, China. Precambrian Research, 174(3-4): 347-363.

Zahirovic, S., Müller, R.D., Seton, M. and Flament, N., 2015. Tectonic speed limits from plate kinematic reconstructions. Earth and Planetary Science Letters, 418: 40-52.

Zhang, N., Zhong, S., Leng, W. and Li, Z., 2010. A model for the evolution of the Earth's mantle structure since the Early Paleozoic. Journal of Geophysical Research, 115(B6): B06401.

Zhang, S., Li, Z.-X., Evans, D.A.D., Wu, H., Li, H. and Dong, J., 2012. Pre-Rodinia supercontinent Nuna shaping up: A global synthesis with new paleomagnetic results from North China. Earth and Planetary Science Letters, 353-354: 145-155.

Zhang, S.-H., Ernst, R.E., Yang, Z., Zhou, Z., Pei, J. and Zhao, Y., 2022. Spatial distribution of 1.4-1.3 Ga LIPs and carbonatite-related REE deposits: Evidence for large-scale continental rifting in the Columbia (Nuna) supercontinent. Earth and Planetary Science Letters, 597.

Zhang, S.-H., Zhao, Y., Li, X.-H., Ernst, R.E. and Yang, Z.-Y., 2017. The 1.33–1.30 Ga Yanliao large igneous province in the North China Craton: Implications for reconstruction of the Nuna (Columbia) supercontinent, and specifically with the North Australian Craton. Earth and Planetary Science Letters, 465: 112-125.

Zhao, G., Cawood, P.A., Wilde, S.A. and Sun, M., 2002. Review of global 2.1–1.8 Ga orogens: implications for a pre-Rodinia supercontinent. Earth-Science Reviews, 59(1-4): 125-162.

Zhao, L., Tyler, I.M., Gorczyk, W., Murdie, R.E., Gessner, K., Lu, Y., Smithies, H., Li, T., Yang, J. and Zhan, A., 2022. Seismic evidence of two cryptic sutures in Northwestern Australia: Implications for the style of subduction during the Paleoproterozoic assembly of Columbia. Earth and Planetary Science Letters, 579: 117342.

Zhao, T., Cawood, P.A., Zi, J.-W., Wang, K., Feng, Q., Tran, D.M., Trinh, H.D., Dang, C.M. and Nguyen, Q.M., 2023. Positioning the Yangtze Block within Nuna: Constraints from Paleoproterozoic granitoids in North Vietnam. Precambrian Research, 391.

Zhu, Z., Campbell, I.H., Allen, C.M., Brocks, J.J. and Chen, B., 2022. The temporal distribution of Earth's supermountains and their potential link to the rise of atmospheric oxygen and biological evolution. Earth and Planetary Science Letters, 580.

Zou, Y., Mitchell, R.N., Chu, X., Brown, M., Jiang, J., Li, Q., Zhao, L. and Zhai, M., 2023. Surface evolution during the mid-Proterozoic stalled by mantle warming under Columbia–Rodinia. Earth and Planetary Science Letters, 607.

Declaration of interests

☒The authors declare that they have no known competing financial interests or personal relationships that could have appeared to influence the work reported in this paper.

☐The authors declare the following financial interests/personal relationships which may be considered as potential competing interests:

Supplementary Figure

Click here to access/download
Supplementary Material
2-Supplementary_material.docx

Supplementary Table 1

Click here to access/download
Supplementary Material
3-TableS1_pmag_poles.xlsx

Supplementary Table 2

Click here to access/download
Supplementary Material
4-TableS2-Accretionary-events.xlsx